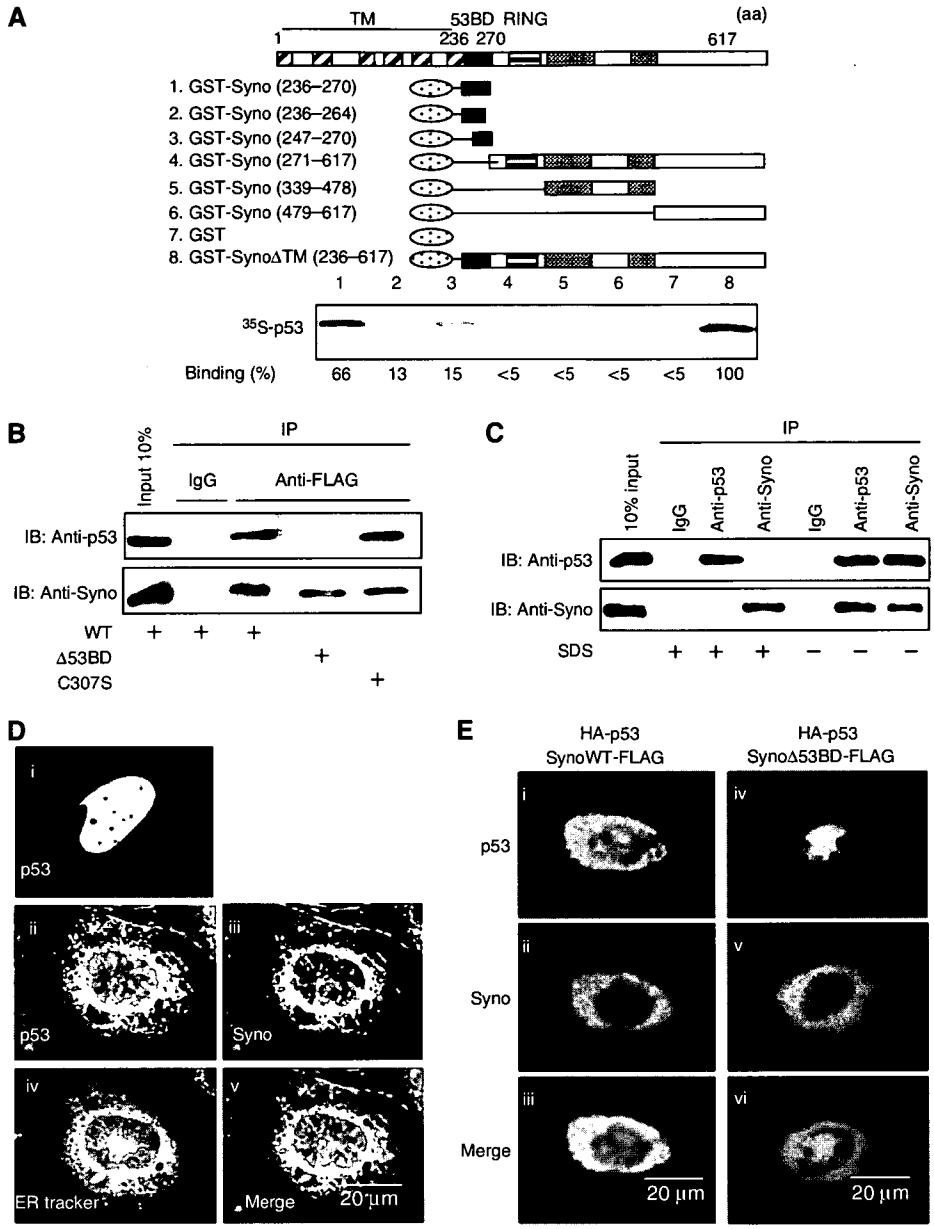

Figure 3 Synoviolin sequestrates p53 in the ER through its 53BD-dependent interaction with p53. (**A**) Identification of p53-binding domain of Synoviolin *in vitro*. Black box: p53-binding domain (53BD), gray box: proline-rich domain, oval box: GST. Relative binding ability is denoted as percentage (100% = SynoΔTM, lane 8). (**B**) 53BD-dependent *in vivo* binding of Synoviolin with p53 in HEK293 cell. (**C**) Interaction between endogenous Synoviolin and p53 in HEK293 cells. Cell lysates were immunoprecipitated in the presence or absence of SDS by using anti-p53 antibodies, anti-Synoviolin antibodies or control IgG. Inputs and immunoprecipitates were analyzed by Western blot by using anti-p53 or anti-Synoviolin antibodies. (**D**) P53 is anchored around ER in a Synoviolin-dependent manner. Saos-2 cells were transfected with HA-p53 (i) or co-transfected with HA-p53 and Synoviolin-FLAG (ii–v). Panel v shows a merged image with p53 (green), Synoviolin (red) and ER-Tracker stain (blue). (**E**) Binding of p53 with Synoviolin is required for p53 anchoring in the ER. Saos-2 cells were co-transfected with HA-p53 and Synoviolin WT-FLAG (I–iii) or SynoviolinΔ53BD-FLAG (iv–vi). Merged images are shown in the bottom panels (iii, vi).

dependent manner, whereas a peptide representing amino acids 322–332 of Synoviolin, used as a negative control, did not show any inhibitory activity (Supplementary Figure 5). We also confirmed *in vivo*, using co-immunoprecipitation assay, the interaction of transiently expressed exogenous Synoviolin WT-FLAG and p53, and the necessity of 53BD was also apparent (Figure 3B). The interaction of these two molecules was independent of ubiquitin ligase activity of Synoviolin, because Synoviolin C307S-FLAG lacking E3 activity bound to p53, as its WT (Figure 3B). Furthermore, endogenous interaction of p53 and Synoviolin was also confirmed in HEK293 cells (Figure 3C).

Considering the interplay between the ER-resident Synoviolin and the nuclear p53, we next investigated their cellular localization in Saos-2 cells, a human osteosarcoma cell line that lacks the endogenous p53 gene (Fogh *et al*, 1977), under conditions of transient expression of exogenous HA-p53 with Synoviolin WT-FLAG or SynoviolinΔ53BD-FLAG (Figure 3D and E). By overexpression of HA-p53 alone in these cells, HA-p53 was localized in the nucleus (Figure 3Di), as reported previously (Shaulsky *et al*, 1990). On the other hand, when HA-p53 was coexpressed with Synoviolin WT-FLAG, HA-p53 was predominantly colocalized with Synoviolin WT-FLAG in the perinuclear regions, but not in

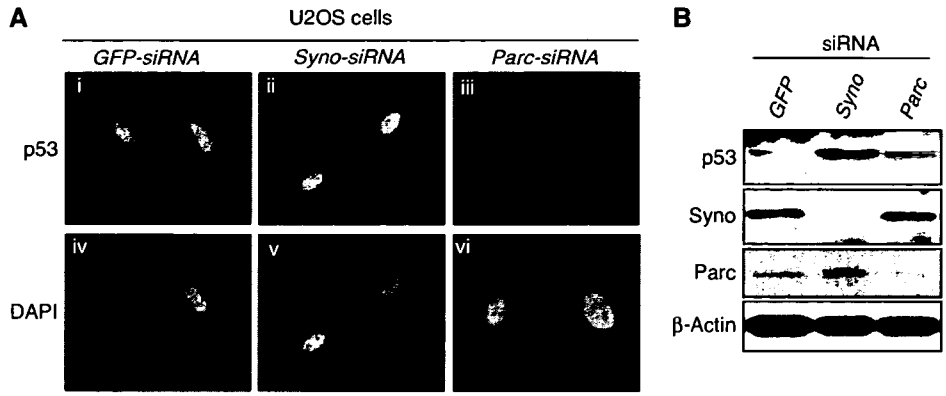

Figure 4 p53-related functional differences between Synoviolin and Parc. (**A**) Nuclear accumulation of p53 by knockdown of *synoviolin* or *Parc*. (**B**) Different levels of p53 following knockdown of *synoviolin* compared with *Parc*.

the nucleus (Figure 3Dii, iii and v). The perinuclear regions were confirmed to be the ER, by counterstaining with ER-Tracker Blue-White DPX (Figure 3Div and v). In addition, ectopically expressed SynoviolinΔ53BD-FLAG did not affect the translocation of HA-p53 into the nucleus (Figure 3E). These results clearly indicate that Synoviolin entraps p53 around ER, and that 53BD is required for this sequestration *in vivo*. In this regard, a previous study reported that another RING finger protein, Parc (Nikolaev *et al*, 2003), also acts as a cytoplasmic anchor for p53. To compare the characteristics of Synoviolin and Parc, we investigated p53 localization in U2OS cells, a human osteosarcoma cell line known to express WT p53 (Ponten and Saksela, 1967), after depletion of *synoviolin* or *Parc* (Nikolaev *et al*, 2003). Treatment with either *Syno* siRNA (Figure 4Aii and v) or *Parc* siRNA (Figure 4Aiii and vi) resulted in accumulation of p53 in the nucleus with diffused and lesser staining in the cytoplasm, different from treatment with *GFP* siRNA. Whereas the nuclear translocation of p53 was comparable in both *Syno* siRNA and *Parc* siRNA cells, a higher expression of p53 was observed in *synoviolin*-deficient U2OS cells (Figure 4Aii and iii). Western blotting analysis also revealed increased level of p53 in Synoviolin-knockdown but not in Parc-knockdown cells (Figure 4B). These findings indicate that Synoviolin regulates both localization and quantity of p53, whereas Parc does not affect the amount of p53, as reported previously (Nikolaev *et al*, 2003).

Synoviolin functions as a novel E3 ubiquitin ligase for p53 degradation

Considering that Synoviolin interacts with p53 *in vitro* and *in vivo*, we next examined whether Synoviolin ubiquitinates p53. As shown in Figure 5A, polyubiquitinated GST-p53 was detected only in the presence of ATP, PK-His-HA-Ub, E1, E2 (UbcH5c) and SynoviolinΔTM (SynoΔTM). This activity was not observed when we used Synoviolin with mutation in the RING finger domain (Figure 5B), and the deletion of 53BD also did not show any ubiquitination activity on p53 (Figure 5B), but this mutant by itself still preserved the auto-ubiquitination activity (Supplementary Figure 6). In addition, the 53BD peptide also inhibited poly-ubiquitination of p53 compared with a control peptide (amino acids 322–332), although the 53BD peptide did not influence the auto-ubiquitination activity of Synoviolin (Supplementary Figure 7). Moreover, ubiquitinated FLAG-p53 was observed when HA-tagged ubiquitin and Synoviolin WT were coexpressed in HEK293 cells because of its easy transfection, but Synoviolin C307S did not (Figure 5C). As a positive control, p53 was ubiquitinated by MDM2 in an *in vivo* ubiquitination assay (Figure 5C) (Haupt *et al*, 1997; Kubbutat *et al*, 1997).

In the next step, we tested the implication of ubiquitination of p53 by Synoviolin in the degradation of p53 *in vivo*. In HEK293 cells, overexpressed Synoviolin WT significantly shortened the half-life of endogenous p53, whereas Synoviolin C307S and SynoviolinΔ53BD did not increase the degradation rate of p53 (Figure 5D top, mock: 125.5±18.2 min, Synoviolin WT: 44.8±3.8 min, Synoviolin C307S: 177.3±26.8 min and SynoviolinΔ53BD: 161.0±41.4 min). These results indicate that Synoviolin is responsible for the turnover of p53 as its E3 ubiquitin ligase *in vivo*. Consistent with these data, the half-life of p53 was significantly prolonged in $Syno^{-/-}$ MEFs (Figure 5D (bottom), $Syno^{+/+}$ MEFs: 26.1±1.6 min; and $Syno^{-/-}$ MEFs: 120.0±30.3 min. $P<0.05$) as well as RKO cells treated with *synoviolin* siRNA (Supplementary Figure 8). In this regard, several ubiquitin ligases, such as *Cop1* (Dornan *et al*, 2004), *Pirh2* (Leng *et al*, 2003) and *MDM2* (Haupt *et al*, 1997; Kubbutat *et al*, 1997), are already reported to negatively regulate p53 (Bode and Dong, 2004). To ascertain the significance of Synoviolin relative to these ligases, we compared the effects of depletion of *synoviolin* and/or *Cop1*, *Pirh2* or *MDM2* on the expression level of p53 in RKO cells. The amount of p53 by *synoviolin* ablation was less than that by *MDM2* ablation, but equivalent to that by *Cop1* ablation. Depletion of *synoviolin* in cells treated with siRNA for *Cop1*, *Pirh2* or *MDM2* non-redundantly increased p53 levels (Figure 5E). Therefore, Synoviolin functionally targets p53 independent of other ubiquitin ligase pathways. Then, does Synoviolin regulate p53 activation process? To address this question, we applied genotoxic stress as a stimulus for p53 activation (Kastan *et al*, 1991; Vogelstein *et al*, 2000). *Syno* siRNA and *GFP* siRNA-transfected RKO cells were treated with or without genotoxic stresses such as camptothecin, actinomycin D and γ-irradiation. As expected, increased level of p53 by Synoviolin knockdown was cooperatively enhanced by treatment with genotoxic stresses in these cells (Figure 5F). Thapsigargin induced Synoviolin expression, as reported previously (Yagishita *et al*, 2005),

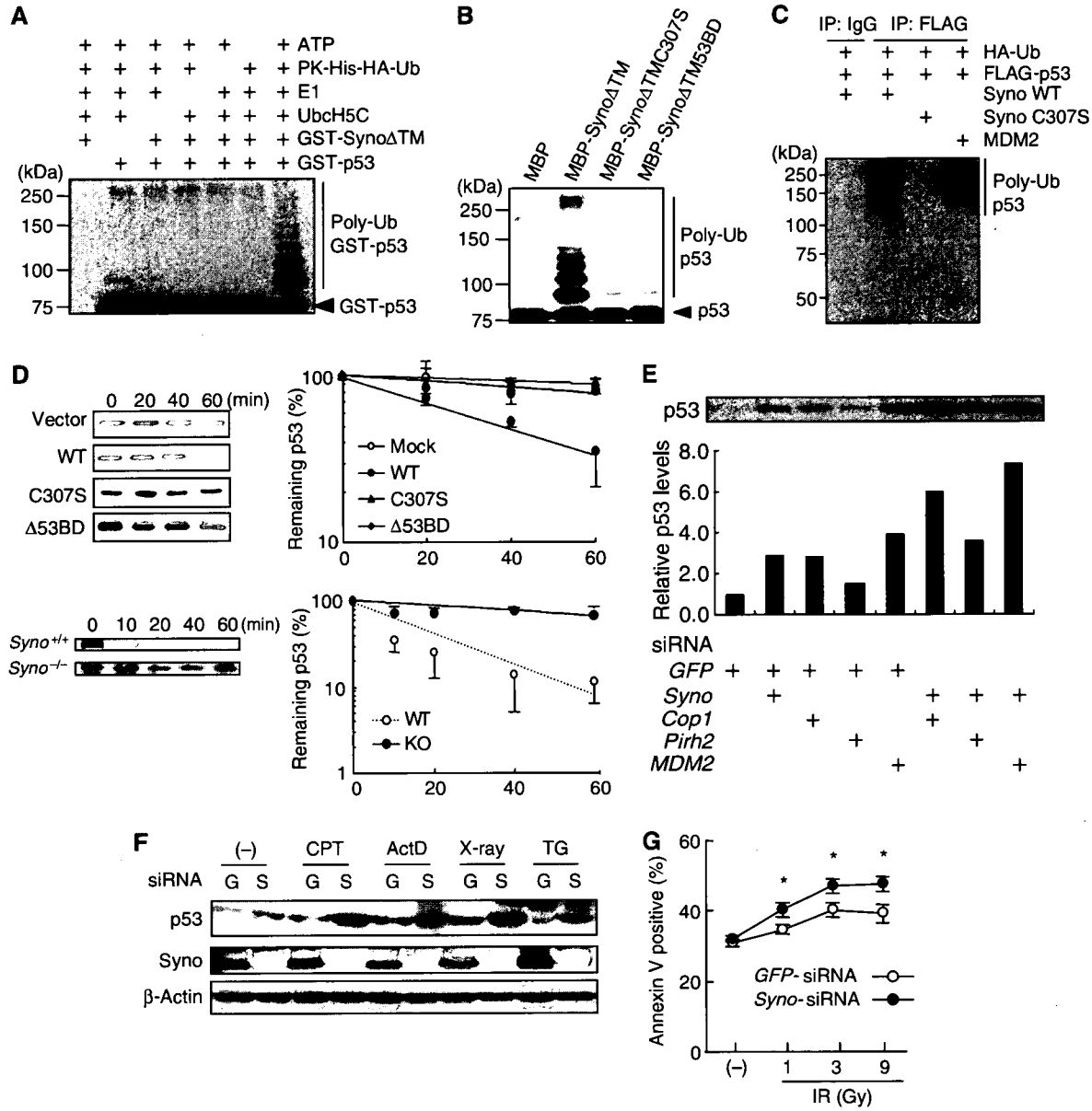

Figure 5 Synoviolin up-regulates p53 level in cells under normal and genotoxic stress conditions. (**A**) Synoviolin ubiquitinates p53 *in vitro*. (**B**) The ubiquitination of p53 is dependent on an intact RING finger domain. (**C**) WT Synoviolin, but not RING finger mutant, ubiquitinates p53 *in vivo*. (**D**) Synoviolin over-expression in HEK293 cells increases degradation of p53 (top). At 24 h after the transfection with empty vector, wild type Synoviolin (WT), mutants in RING finger domain (C307S) or p53 binding domain deletion mutant (Δ53BD), p53 expression was examined at indicated time of cycloheximide treatment. Degradation of p53 is inhibited in synoviolin knockout MEFs ($Syno^{-/-}$) compared with wild type MEFs ($Syno^{+/+}$). The p53 expression was examined after the indicated time of cycloheximide treatment. The remaining p53 expressions were normalized to β-actin expression and plotted against time (minutes). (**E**) Effects of knockdown of Synoviolin and/or other known E3 ubiquitin ligases for p53 on the level of p53 in RKO cells. Quantified p53 level is expressed as relative levels (1.0 = *GFP*-siRNA treated RKO cells). (**F**) Genotoxic stress induces p53 accumulation in the absence of Synoviolin. *GFP*- siRNA (G). *syno* siRNA (S). At 48 h after transfection, the RKO cells were treated with vehicle, camptothecine (CPT, 0.5 μM), actinomycin D (ActD, 5 nM), X-Ray (9 Gray) or thapsigargin (TG, 1 μM) for 6 h. (**G**) Synoviolin knockdown sensitizes cells to genotoxic stress. At 48 h after transfection, cells were exposed to the indicated doses of ionizing-radiation for 24 h, followed by FACS analysis to detect annexin V-positive cells. Data in (D) and (G) are mean ± s.e.m. of $n \geqslant 3$. $^*P < 0.05$.

which was abolished in *Syno* siRNA-transfected RKO cells (Figure 5F). Consistent with the findings of a previous report (Qu *et al*, 2004), thapsigargin, an ER stress inducer, destabilized p53 expression compared with vehicle treatment in *GFP* siRNA-treated RKO cells. Interestingly, the thapsigargin-induced inhibition of p53 expression was reversed, at least in part, by the ablation of Synoviolin (Figure 5F). In addition, the sensitivity of *syno* siRNA-treated RKO cells to γ-irradiation was significantly increased compared with *GFP* siRNA-treated RKO cells (Figure 5G). Considered together, these results indicate that Synoviolin also participates in genotoxic stress response through the mechanism identified here.

Synoviolin regulates p53-dependent apoptotic pathway in vivo

The above experiments provided several pieces of evidence that Synoviolin is a novel class of E3 ubiquitin ligase for p53. However, the majority of the results obtained from cultured cells may not fully reflect the physiological function of p53 in

the context of the whole organism. Therefore, we used *Drosophila* to confirm the association between Synoviolin and p53. Among *Drosophila* clones, CG1937 was identified by BLASTP (protein-protein blast analysis using flybase—http://flybase.bio.indiana.edu/blast/) as the gene with 63% homology to mammalian Synoviolin, and the RING domain of CG1937 is highly conserved (82%) and *in vitro* ubiquitination assay evidently indicated that *Drosophila* Synoviolin (dSyno) ubiquitinates *Drosophila* p53 (Dmp53) (Figure 6A) (Ollmann *et al*, 2000). To investigate the role of Synoviolin in p53 regulation in the whole organism, we generated transgenic flies in which Dmp53 or dSyno was overexpressed by tissue-specific Gal4 driver (Harrison *et al*, 1995). By crossing each transgenic fly, we generated e16E-Gal4/UAS-Dmp53;UAS-dSyno/+ flies, in which both Dmp53 and dSyno could be overexpressed in the posterior halves of wings by e16E-Gal4 driver. The expression level of Dmp53 in the wing discs was significantly decreased in e16E-Gal4/UAS-Dmp53;UAS-dSyno/+ discs compared with e16E-Gal4/Dmp53;+/+ discs (Figure 6B). Moreover, acridine orange staining of apoptotic cells in these discs demonstrated that the level of apoptosis induced by overexpression of Dmp53 was diminished by dSyno overexpression (Figure 6C). These results indicate that dSyno affects Dmp53 protein levels in the fly system, similar to the results of the cell culture system.

In addition to decreased Dmp53 protein level by dSyno in the wing discs of adult flies, dSyno altered the wing phenotype. Namely, overexpression of Dmp53 by e16E-Gal4 driver caused bubbled wing phenotype at the posterior half of wings (Figure 6Di). This phenotype was completely suppressed by dSyno overexpression (Figure 6Dii and Supplementary Table 1). Overexpression of dSyno alone by e16E-Gal4 driver also produced wing phenotype (weak wrinkling of the posterior edge of the wing) (Figure 6Diii). This wrinkled phenotype

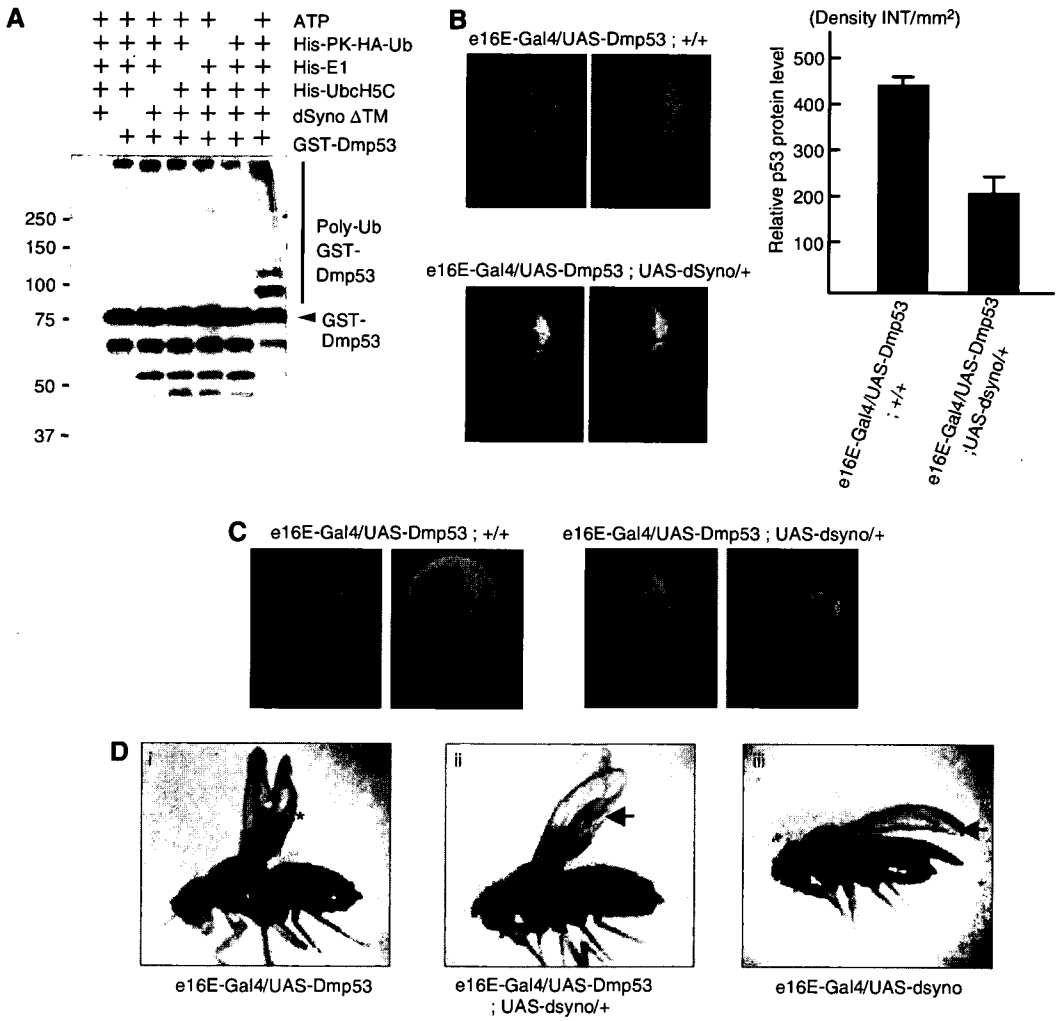

Figure 6 Synoviolin directly regulates p53-dependent apoptotic pathway in *Drosophila* fly. (**A**) Fly homolog of Synoviolin ubiquitinates fly homolog of p53 *in vitro*. GST-fusion *Drosophila melanogaster* p53 (Dmp53) was incubated with or without ATP, His-PK-HA-Ub, His-E1 (human), His-UbcH5C (human) and *Drosophila* Synoviolin (dSyno)ΔTM. Ubiquitinated proteins were probed with anti-HA antibody. (**B**) P53 protein level of wing discs was determined by immunostaining using anti-Dmp53 antibody (left). 2 representative pictures of each fly are shown. The fluorescence intensity of each 15 fly disc was quantified, and the net density level (Density INT/mm^2) was determined by subtracting the density level of the background area (anterior half of disc) from the measured level of the target area (posterior half of disc) (right). Data are mean ± s.e.m. of $n = 15$. (**C**) Apoptosis was examined by Acridine orange staining of wing disc. Overexpression of dSyno in the posterior half of the discs reduced Dmp53 overexpression-induced apoptosis. (**D**) Overexpression of dSyno suppressed the Dmp53-induced bubbled wing phenotype. The extent of wing bubble (*) in e16E-Gal4/UAS-Dmp53 flies varied with age, but the penetrance of bubbled wing phenotype was close to 100% (Supplementary Table 1). Overexpression of dSyno suppressed the Dmp53-induced bubbled wing phenotype, but dSyno-induced wrinkled phenotype at the posterior edge of wing was still observed (arrow).

induced by dSyno overexpression was not affected by Dmp53 in the double overexpressing flies (Figure 6Dii and iii, arrow). These results confirm that dSyno regulates Dmp53 protein level *in vivo* and such regulation might be accomplished through ubiquitination of dDmp53.

To determine whether this phenotypic suppression of Dmp53 by dSyno is specific to Dmp53, we investigated the interaction between dSyno and the upstream activators of p53 such as dATM, CHK2, using the same strategy. None of these activators showed interaction with dSyno (data not shown), suggesting that dSyno regulates Dmp53 protein level directly *in vivo*.

Discussion

We provide concrete evidence for the first time of the functional relationship between Synoviolin and p53. As a target for Synoviolin, p53 is evidently a non-ERAD substrate. In this regard, Doa10p, the RING finger E3 ubiquitin ligase, is known not only to be involved exclusively in removing ER proteins in the ERAD, but also to eliminate cytoplasmic targets, especially the soluble transcriptional factor Matα2, which translocates into the nucleus similar to p53 (Swanson *et al*, 2001; Laney and Hochstrasser, 2003). Thus, our finding can be viewed within the same framework of yeast though in higher eukaryotes. In the meantime, it was proposed that the ERAD in yeast is composed of two distinct surveillance mechanisms, that is, the folded state of luminal domains and the cytosolic domains are monitored by ERAD-luminal (ERAD-L) and ERAD-cytosolic (ERAD-C) pathways, respectively (Vashist and Ng, 2004; Nishikawa *et al*, 2005). Hrd1p is recognized as an ERAD-L ligase; however, this classification is not applicable to Synoviolin as a human homolog of yeast Hrd1, because Synoviolin can target both ERAD-L substrate and cytoplasmic p53 (ERAD-C substrate). Therefore, we propose the novel regulatory system of Synoviolin as a different classification of the ERAD-L/C pathway.

Maintenance of homeostasis is an important cellular function, and cells are equipped with various processes to maintain their conditions. Transcriptional alteration mediated by p53 results in a variety of cell fate changes, including growth arrest and apoptosis (Vousden and Lu, 2002; Meek, 2004). Normally, the cell maintains low levels of p53 through rapid protein degradation via the UPS by the function of ubiquitin ligases. In contrast, under genotoxic stress conditions, stabilization of p53 is promoted and the diffusely distributed p53 translocates to the nucleus owing to growth inhibition and apoptosis by its transcriptional activity. Thus, adjusting the level and nuclear localization of p53 are two essential processes for cells in order to maintain the physiological state. Although p53 mutations have been documented in more than half of all human tumors (Hollstein *et al*, 1999), it is also known that tumor cells retain WT p53. In this regard, functional inactivation of WT p53 by abnormal cytoplasmic sequestration is frequently observed in many tumor types (Moll *et al*, 1992, 1996; Schlamp *et al*, 1997). The RING finger protein Parc is considered to act as a cytoplasmic anchoring molecule of p53, but this clone does not have a p53 ubiquitination activity (Nikolaev *et al*, 2003). On the other hand, our present findings demonstrated that Synoviolin not only anchors p53 in the cytoplasm, but also ubiquitinates it, and thus differs from Parc (Figure 4). Moreover, Synoviolin diverges from other ligases for p53; each of the three ubiquitin ligases for p53 (MDM2, Pirh2 and Cop1) forms an autoregulatory negative feedback loop, resulting in lower p53 activity upon its expression, but these three ligases are target for the p53 transcriptional pathway (Dornan *et al*, 2004; Leng *et al*, 2003), whereas the expression of Synoviolin is not regulated by p53 (Figure 5F). Indeed, the *synoviolin* promoter region does not have a p53 target sequence, whereas it contains the ER stress responsive element (Tsuchimochi *et al*, 2005) and responds to the stress (Figure 5F). The reason for the multiple post-translational steps for p53 is the enormous importance of this molecule in maintaining cellular homeostasis. p53 is negatively regulated by various ubiquitin ligases, such as MDM2, MdmX, HAUSP, ARF, COP1, Pirh2 and ARF-BP1 (Brooks and Gu, 2006), and it is assumed that each molecule has its specific roles in p53 control. Among them, Synoviolin is also a unique regulator of p53 because of its independency from other ligases and transcriptional regulation by p53, ER localization and canonical function in ERAD.

In the present study, we demonstrated that Synoviolin participates in genotoxic stress-mediated p53 signaling, and its to participation in the ER stress-induced apoptosis is also well known (Bordallo *et al*, 1998; Kaneko *et al*, 2002; Kikkert *et al*, 2004; Yagishita *et al*, 2005). Therefore, Synoviolin seems to regulate two distinct apoptotic pathways and the ubiquitination of p53 by Synoviolin may be another target for crosstalk between them. Another linkage between ER stress and p53 pathway is also implicated by our finding that UPR markers are increased in cells with *synoviolin* knockdown (data not shown). Two reports described a crosstalk of p53- and ER stress- induced apoptosis pathways, that is, ER stress antagonizes p53-mediated apoptosis through the cytoplasmic localization of p53 due to phosphorylation by glycogen synthase kinase-3β (GSK-3β) (Qu *et al*, 2004), and p53 destabilization utilized the cooperative action of MDM2 and GSK-3β in ER-stressed cells (Pluquet *et al*, 2005). In this regard, it is important to note that UPR activation upon Synoviolin knockdown in RKO cells may be related to ER stress with impaired ERAD system. Since Synoviolin null cells show upregulation of p53, it is possible that the effect of p53 stabilization by Synoviolin knockdown exceeds the p53 destabilization effect of UPR induced by Synoviolin knockdown. This hypothesis may be supported by the finding that *synoviolin* siRNA treatment seemed to restore the expression of p53 at least in part, which was suppressed by ER stress (Figure 5F). The regulatory action of Synoviolin on p53 under ER stress is obviously more complex, because ER stress also induces Synoviolin expression. Further studies are necessary to determine the physiological regulatory role of Synoviolin in p53 expression under ER stress conditions.

The function of p53 in patients with RA is still controversial (Firestein *et al*, 1997; Reme *et al*, 1998; Inazuka *et al*, 2000; Muller-Ladner and Nishioka, 2000; Sun and Cheung, 2002). Mice lacking p53 do not develop spontaneous arthropathy but have severe collagen-induced arthritis (CIA) (Yamanishi *et al*, 2002; Simelyte *et al*, 2005). As we reported previously, overexpression of Synoviolin resulted in spontaneous arthropathy and its deficiency resulted in resistance to CIA in mice (Amano *et al*, 2003). Therefore, we assumed that the severity of arthritis could be determined by the Synoviolin–p53 control pathway and that the onset of spon-

taneous arthropathy may be caused by p53-independent pathway in these models. The influence of these relationships on arthritis is currently being examined in our laboratories, using *synoviolin* and p53 double null mutant mice. We hope that our research could uncover new pathogenic mechanisms of RA. Furthermore, since p53 is an important tumor suppressor gene, we believe that Synoviolin could be a useful therapeutic target for not only RA but also cancer based on its cytological and biochemical features, i.e., cytoplasmic localization and enzymatic activity (Hopkins and Groom, 2002).

In conclusion, we demonstrated that Synoviolin acts as an ERAD E3 ubiquitin ligase that controls cellular p53 and thus opens, a new concept for proliferative disorders such as RA and cancer.

Materials and methods

Plasmids

pcDNA3/Synoviolin WT or C307S-FLAG, pcDNA3/HA- and FLAG-p53, pcDNA3/MDM2 and pcDNA/HA-Ub plasmids have been described previously (Amano *et al*, 2003; Matsushita *et al*, 2005). Deletion of 53BD, MBP- and GST-fusions in Synoviolin deletion mutants was performed by PCR-based method in this study. To clone a cDNA encoding *Drosophila* homolog of human Synoviolin (dSyno), 2282 bp of CG1937 was cut out from EST GH11117 with *EcoRI*/*XhoI*, and subcloned into pUAST vector (Brand and Perrimon, 1993). The sequences of all plasmids generated by PCR were confirmed by ABI auto-sequencer.

Cells and transfections

RKO and HEK293 cells were cultured in Minimum Essential Medium (Sigma) and U2OS and Saos-2 in Dulbecco's modified Eagle's medium (Sigma). The sense sequences of siRNA oligonucleotides to *synoviolin* are (1) GGUGUUCUUUGGGCAACUG, (2) GCUGUGACAGAUGCCAUCA, (3) GGUUCUGCUGUACAUGGCC. Changes in p53 protein in RKO cells were determined by all these siRNAs. The sense sequence of siRNA oligonucleotides to *GFP* is GGCUACGUCCAGGAGCGC.

GST pull-down assay

GST-fusion proteins were expressed in *Escherichia coli* strain BL21 (Invitrogen) and purified by using glutathione-Sepharose beads (Amersham Biosciences). *In vitro*-translated ^{35}S-labeled p53 was pre-cleaned with 10 μg GST protein for 1 h at 4°C, followed by incubation with 10 μg of each GST-fusion protein in binding buffer (20 mM *N*-2-hydroxyethylpiperazine-*N'*-ethanesulfonic acid (HEPES), pH 7.9, 150 mM NaCl and 0.2% TritonX-100) for 1 h at 4°C. After washing, bound proteins were separated by SDS–PAGE and detected by BAS.

Immunoprecipitation assay

For co-immunoprecipitation assay between exogenous Synoviolin and exogenous p53, HEK293 cells were co-transfected with HA-p53 and pcDNA3-Synoviolin WT-FLAG, pcDNA3-SynoviolinΔ53BD-FLAG or pcDNA3-Synoviolin C307S-FLAG plasmids. Cell extracts were prepared with high-salt buffer (20 mM HEPES pH 7.2, 420 mM NaCl, 10% glycerol, 0.5% NP-40, 0.5 mM dithiothreitol (DTT), and 1 mM phenylmethylsulfonyl fluoride (PMSF)) and diluted at three-fold with 0.5 mM DTT and a protease inhibitor solution, followed by incubation with mouse IgG or anti-FLAG antibody. Precipitated proteins were detected by anti-HA or anti-FLAG antibodies.

To detect the interaction between endogenous Synoviolin and p53, HEK293 cells were lysed in 100 mM Tris–HCl, 80 mM NaCl, 1 mM EDTA, 5 mM EGTA, 5% glycerol, 2% (w/v) digitonin, 0.1% Brij 35, protease inhibitor cocktail and 20 μM of MG132. Immunoprecipitation was carried out in the presence or absence of SDS by using anti-p53 antibodies, anti-Synoviolin antibodies or control IgG. The immunoprecipitated samples were analyzed by western blot by using anti-p53 or anti-Synoviolin antibodies.

In vitro and in vivo ubiquitination assays

The *in vitro* ubiquitination assay was conducted as described previously (Amano *et al*, 2003). For the peptide inhibition assay, reaction solutions lacking no MBP-SynoviolinΔTM-6xHis and ATP were incubated with 53BD or control peptides (50, 100, and 200 μM) for 30 min at 4°C. Reactions were started by addition of MBP-SynoviolinΔTM-6xHis and ATP and incubating at 37°C.

For the *in vivo* ubiquitination assay, HEK293 cells were transfected with pcDNA3/HA-Ubiquitin, pcDNA3/FLAG-p53, and pcDNA3/Synoviolin WT, C307S or pcDNA3/MDM2. At 24 h post-transfection, cells were treated with MG132 (10 μM) for 1 h, then the cells were lysed in SDS containing buffer (50 mM Tris, pH 7.5, 0.5 mM EDTA, 1% SDS, and 1 mM DTT) and boiled for 5 min to denature the proteins. The denatured samples were diluted with immunoprecipitation buffer (50 mM Tris, pH 7.5, 2 mM EDTA, 150 mM NaCl, and 0.1% NP-40 and protease inhibitor cocktail) and the p53 protein was immunopurified by using anti-p53 antibody. Ubiquitinated p53 was detected by western blotting by using anti-HA antibody.

Immunostaining of fly wing discs

Fly wing discs were dissected in PBS, fixed in a buffer containing 50 mM Tris–HCl, pH 6.8, 1 mM EGTA, 1% Triton ×-100, 2 mM $MgSO_4$, 150 mM NaCl, and 2.2% formaldehyde for 15 min, and blocked using a blocking buffer (50 mM Tris–HCl, pH 6.8, 150 mM NaCl, 0.5% NP-40 and 5 mg/ml BSA). The fixed wing discs were incubated overnight at 4°C in a 1:200 dilution of anti-Dmp53 (d-200) antibody. After washing in a wash buffer (50 mM Tris–HCl, pH 6.8, 150 mM NaCl, 0.5% NP-40 and 1 mg/ml BSA), they were incubated for 3 h at 4°C in donkey anti-rabbit FITC at 1:200 dilution, washed with the wash buffer and then mounted in a mounting solution (50 mM Tris–HCl, pH 6.8, 30% glycerol, 150 mM NaCl, and 5 mg/ml phenylethylendiamine). The fluorescence intensity of each disc was quantified with Quantity One software (Bio-Rad Laboratories). Acridine orange staining was performed as reported previously (Brodsky *et al*, 2000).

Supplementary data

Supplementary data are available at *The EMBO Journal* Online (http://www.embojournal.org).

Acknowledgements

We are grateful to MR Montminy, G Verdine, R Nagata, H Shimizu, I Hishinuma, H Yokohama, H Kato, S Kitamura, K Yoshimatsu, Yuichiro ITAKURA OFFICE and ES Takagi, for advice and encouragement, and to H Takahashi, M Sato, S Otani, A Sugamiya, N Takagi, S Shinkawa, Y Nakagawa, Y Sato, M Yamanashi and members of Toshi's Laboratory for the excellent technical assistance. This study was supported in part by LocomoGene Inc., Eisai Co., Ltd, National Institute of Biomedical Innovation, the Japanese Ministry of Education, Culture, Sports, Science and Technology, the Japanese Ministry of Health, Labour and Welfare, the Kato Memorial Trust for Nanbyo Research, the Japan Medical Association, Nagao Memorial Fund, Kanae Foundation for Life & Socio-medical Science, Japan Research Foundation for Clinical Pharmacology, Kanagawa Nanbyo Foundation, Kanagawa Academy of Science and Technology Research Grants, Japan College of Rheumatology, the Nakajima Foundation, Japan Society for Promotion of Science, New Energy and Industrial Technology Development Organization, Mochida Pharmaceutical Co. Ltd, Kanto Bureau of Economy, Trade and Industry, and the Uehara Memorial Foundation. HF is supported by Japan Society for the Promotion of Science.

References

Amano T, Yamasaki S, Yagishita N, Tsuchimochi K, Shin H, Kawahara K, Aratani S, Fujita H, Zhang L, Ikeda R, Fujii R, Miura N, Komiya S, Nishioka K, Maruyama I, Fukamizu A, Nakajima T (2003) Synoviolin/Hrd1, an E3 ubiquitin ligase, as a novel pathogenic factor for arthropathy. *Genes Dev* **17**: 2436–2449

Bode AM, Dong Z (2004) Post-translational modification of p53 in tumorigenesis. *Nat Rev Cancer* **4**: 793–805

Bordallo J, Plemper RK, Finger A, Wolf DH (1998) Der3p/Hrd1p is required for endoplasmic reticulum-associated degradation of misfolded lumenal and integral membrane proteins. *Mol Biol Cell* **9:** 209–222

Brand AH, Perrimon N (1993) Targeted gene expression as a means of altering cell fates and generating dominant phenotypes. *Development* **118:** 401–415

Brodsky MH, Nordstrom W, Tsang G, Kwan E, Rubin GM, Abrams JM (2000) *Drosophila* p53 binds a damage response element at the reaper locus. *Cell* **101:** 103–113

Brooks CL, Gu W. (2006) p53 ubiquitination: Mdm2 and beyond. *Mol Cell* **21:** 307–315

Dornan D, Wertz I, Shimizu H, Arnott D, Frantz GD, Dowd P, O'Rourke K, Koeppen H, Dixit VM (2004) The ubiquitin ligase COP1 is a critical negative regulator of p53. *Nature* **429:** 86–92

Firestein GS, Echeverri F, Yeo M, Zvaifler NJ, Green DR (1997) Somatic mutations in the p53 tumor suppressor gene in rheumatoid arthritis synovium. *Proc Natl Acad Sci USA* **94:** 10895–10900

Fogh J, Wright WC, Loveless JD (1977) Absence of HeLa cell contamination in 169 cell lines derived from human tumors. *J Natl Cancer Inst* **58:** 209–214

Gottlieb E, Haffner R, King A, Asher G, Gruss P, Lonai P, Oren M (1997) Transgenic mouse model for studying the transcriptional activity of the p53 protein: age- and tissue-dependent changes in radiation-induced activation during embryogenesis. *EMBO J* **16:** 1381–1390

Harrison DA, Binari R, Nahreini TS, Gilman M, Perrimon N (1995) Activation of a *Drosophila* Janus kinase (JAK) causes hematopoietic neoplasia and developmental defects. *EMBO J* **14:** 2857–2865

Haupt Y, Maya R, Kazaz A, Oren M (1997) Mdm2 promotes the rapid degradation of p53. *Nature* **387:** 296–299

Hershko A, Ciechanover A (1998) The ubiquitin system. *Annu Rev Biochem* **67:** 425–479

Hollstein M, Hergenhahn M, Yang Q, Bartsch H, Wang ZQ, Hainaut P (1999) New approaches to understanding p53 gene tumor mutation spectra. *Mutat Res* **431:** 199–209

Hopkins AL, Groom CR (2002) The druggable genome. *Nat Rev Drug Discov* **1:** 727–730

Inazuka M, Tahira T, Horiuchi T, Harashima S, Sawabe T, Kondo M, Miyahara H, Hayashi K (2000) Analysis of p53 tumour suppressor gene somatic mutations in rheumatoid arthritis synovium. *Rheumatology* **39:** 262–266

Kaneko M, Ishiguro M, Niinuma Y, Uesugi M, Nomura Y (2002) Human HRD1 protects against ER stress-induced apoptosis through ER-associated degradation. *FEBS Lett* **532:** 147–152

Kastan MB, Onyekwere O, Sidransky D, Vogelstein B, Craig RW (1991) Participation of p53 protein in the cellular response to DNA damage. *Cancer Res* **51:** 6304–6311

Kikkert M, Doolman R, Dai M, Avner R, Hassink G, vanVoorden S, Thanedar S, Roitelman J, Chau V, Wiertz E (2004) Human HRD1 is an E3 ubiquitin ligase involved in degradation of proteins from the endoplasmic reticulum. *J Biol Chem* **279:** 3525–3534

Kubbutat MH, Jones SN, Vousden KH (1997) Regulation of p53 stability by Mdm2. *Nature* **387:** 299–303

Laney JD, Hochstrasser M (2003) Ubiquitin-dependent degradation of the yeast Mat(alpha)2 repressor enables a switch in developmental state. *Genes Dev* **17:** 2259–2270

Leng RP, Lin Y, Ma W, Wu H, Lemmers B, Chung S, Parant JM, Lozano G, Hakem R, Benchimol S (2003) Pirh2, a p53-induced ubiquitin-protein ligase, promotes p53 degradation. *Cell* **112:** 779–791

Matsushita N, Kitao H, Ishiai M, Nagashima N, Hirano S, Okawa K, Ohta T, Yu DS, McHugh PJ, Hickson ID, Venkitaraman AR, Kurumizaka H, Takata M (2005) A FancD2-Monoubiquitin Fusion Reveals Hidden Functions of Fanconi Anemia Core Complex in DNA Repair. *Mol Cell* **19:** 841–847

Meek DW (2004) The p53 response to DNA damage. *DNA Repair* **3:** 1049–1056

Moll UM, Ostermeyer AG, Haladay R, Winkfield B, Frazier M, Zambetti G (1996) Cytoplasmic sequestration of wild-type p53 protein impairs the G1 checkpoint after DNA damage. *Mol Cell Biol* **16:** 1126–1137

Moll UM, Riou G, Levine AJ (1992) Two distinct mechanisms alter p53 in breast cancer: mutation and nuclear exclusion. *Proc Natl Acad Sci USA* **89:** 7262–7266

Muller-Ladner U, Nishioka K (2000) p53 in rheumatoid arthritis: friend or foe? *Arthritis Res* **2:** 175–178

Nikolaev AY, Li M, Puskas N, Qin J, Gu W (2003) Parc: a cytoplasmic anchor for p53. *Cell* **112:** 29–40

Nishikawa S, Brodsky JL, Nakatsukasa K (2005) Roles of molecular chaperones in endoplasmic reticulum (ER) quality control and ER-associated degradation (ERAD). *J Biochem* **137:** 551–555

Ollmann M, Young LM, Di Como CJ, Karim F, Belvin M, Robertson S, Whittaker K, Demsky M, Fisher WW, Buchman A, Duyk G, Friedman L, Prives C, Kopczynski C (2000) *Drosophila* p53 is a structural and functional homolog of the tumor suppressor p53. *Cell* **101:** 91–101

Pickart CM (2001) Mechanisms underlying ubiquitination. *Annu Rev Biochem* **70:** 503–533

Pluquet O, Qu L, Baltzis D, Koromilas AE (2005) Endoplasmic reticulum stress accelerates p53 degradation by the cooperative actions of Hdm2 and Glycogen synthase kinase 3β. *Mol Cell Biol* **25:** 9392–9405

Ponten J, Saksela E (1967) Two established *in vitro* cell lines from human mesenchymal tumours. *Int J Cancer* **2:** 434–447

Qu L, Huang S, Baltzis D, Rivas-Estilla AM, Pluquet O, Hatzoglou M, Koumenis C, Taya Y, Yoshimura A, Koromilas AE (2004) Endoplasmic reticulum stress induces p53 cytoplasmic localization and prevents p53-dependent apoptosis by a pathway involving glycogen synthase kinase-3beta. *Genes Dev* **18:** 261–277

Reme T, Travaglio A, Gueydon E, Adla L, Jorgensen C, Sany J (1998) Mutations of the p53 tumour suppressor gene in erosive rheumatoid synovial tissue. *Clin Exp Immunol* **111:** 353–358

Schlamp CL, Poulsen GL, Nork TM, Nickells RW (1997) Nuclear exclusion of wild-type p53 in immortalized human retinoblastoma cells. *J Natl Cancer Inst* **89:** 1530–1536

Shaulsky G, Goldfinger N, Ben-Ze'ev A, Rotter V (1990) Nuclear accumulation of p53 protein is mediated by several nuclear localization signals and plays a role in tumorigenesis. *Mol Cell Biol* **10:** 6565–6577

Shearer AG, Hampton RY (2004) Structural control of endoplasmic reticulum-associated degradation: effect of chemical chaperones on 3-hydroxy-3-methylglutaryl-CoA reductase. *J Biol Chem* **279:** 188–196

Shearer AG, Hampton RY (2005) Lipid-mediated, reversible misfolding of a sterol-sensing domain protein. *EMBO J* **24:** 149–159

Simelyte E, Rosengren S, Boyle DL, Corr M, Green DR, Firestein GS (2005) Regulation of arthritis by p53: Critical role of adaptive immunity. *Arthritis Rheum* **52:** 1876–1884

Smith ML, Chen IT, Zhan Q, O'Connor PM, Fornace Jr AJ (1995) Involvement of the p53 tumor suppressor in repair of u.v.-type DNA damage. *Oncogene* **10:** 1053–1059

Sun Y, Cheung HS (2002) p53, proto-oncogene and rheumatoid arthritis. *Semin Arthritis Rheum* **31:** 299–310

Swanson R, Locher M, Hochstrasser M (2001) A conserved ubiquitin ligase of the nuclear envelope/endoplasmic reticulum that functions in both ER-associated and Matalpha2 repressor degradation. *Genes Dev* **15:** 2660–2674

Tsuchimochi K, Yagishita N, Yamasaki S, Amano T, Kato Y, Kawahara K, Aratani S, Fujita H, Ji F, Sugiura A, Izumi T, Sugamiya A, Maruyama I, Fukamizu A, Komiya S, Nishioka K, Nakajima T (2005) Identification of a crucial site for synoviolin expression. *Mol Cell Biol* **25:** 7344–7356

Vashist S, Ng DT (2004) Misfolded proteins are sorted by a sequential checkpoint mechanism of ER quality control. *J Cell Biol* **165:** 41–52

Vogelstein B, Lane D, Levine AJ (2000) Surfing the p53 network. *Nature* **408:** 307–310

Vousden KH, Lu X (2002) Live or let die: the cell's response to p53. *Nat Rev Cancer* **2:** 594–604

Wu J, Kaufman RJ (2006) From acute ER stress to physiological roles of the Unfolded Protein Response. *Cell Death Differ* **13:** 374–384

Yagishita N, Ohneda K, Amano T, Yamasaki S, Sugiura A, Tsuchimochi K, Shin H, Kawahara K, Ohneda O, Ohta T, Tanaka S, Yamamoto M, Maruyama I, Nishioka K, Fukamizu A, Nakajima T (2005) Essential role of synoviolin in embryogenesis. *J Biol Chem* **280:** 7909–7916

Yamanishi Y, Boyle DL, Pinkoski MJ, Mahboubi A, Lin T, Han Z, Zvaifler NJ, Green DR, Firestein GS (2002) Regulation of joint destruction and inflammation by p53 in collagen-induced arthritis. *Am J Pathol* **160:** 123–130

Intestinal Lamina Propria Retaining $CD4^+CD25^+$ Regulatory T Cells Is A Suppressive Site of Intestinal Inflammation[1]

Shin Makita,* Takanori Kanai,[2]* Yasuhiro Nemoto,* Teruji Totsuka,* Ryuichi Okamoto,* Kiichiro Tsuchiya,* Masafumi Yamamoto,† Hiroshi Kiyono,‡ and Mamoru Watanabe*

It is well known that immune responses in the intestine remain in a state of controlled inflammation, suggesting that not only does active suppression by regulatory T (T_{REG}) cells play an important role in the normal intestinal homeostasis, but also that its dysregulation of immune response leads to the development of inflammatory bowel disease. In this study, we demonstrate that murine $CD4^+CD25^+$ T cells residing in the intestinal lamina propria (LP) constitutively express CTLA-4, glucocorticoid-induced TNFR, and Foxp3 and suppress proliferation of responder $CD4^+$ T cells in vitro. Furthermore, cotransfer of intestinal LP $CD4^+CD25^+$ T cells prevents the development of chronic colitis induced by adoptive transfer of $CD4^+CD45RB^{high}$ T cells into SCID mice. When lymphotoxin (LT)α-deficient intercrossed Rag2 double knockout mice ($LT\alpha^{-/-} \times Rag2^{-/-}$), which lack mesenteric lymph nodes and Peyer's patches, are transferred with $CD4^+CD45RB^{high}$ T cells, they develop severe wasting disease and chronic colitis despite the delayed kinetics as compared with the control $LT\alpha^{+/+} \times Rag2^{-/-}$ mice transferred with $CD4^+CD45RB^{high}$ T cells. Of note, when a mixture of splenic $CD4^+CD25^+$ T_{REG} cells and $CD4^+CD45RB^{high}$ T cells are transferred into $LT\alpha^{-/-} \times Rag2^{-/-}$ recipients, $CD4^+CD25^+$ T_{REG} cells migrate into the colon and prevent the development of colitis in $LT\alpha^{-/-} \times Rag2^{-/-}$ recipients as well as in the control $LT\alpha^{+/+} \times Rag2^{-/-}$ recipients. These results suggest that the intestinal LP harboring $CD4^+CD25^+$ T_{REG} cells contributes to the intestinal immune suppression. *The Journal of Immunology,* 2007, 178: 4937–4946.

Intestinal mucosal surfaces are exposed to alimentary and bacterial Ags of the intestinal flora (1). The gut-associated immune system fences off potentially harmful intestinal Ags from systemic circulation and induces systemic tolerance against luminal Ags. In contrast, inflammatory bowel disease is associated with activation of the local intestinal and systemic immune responses (2, 3). $CD4^+CD25^+$ regulatory T (T_{REG})[3] cells fulfill a central role in the maintenance of immunological homeostasis and self-tolerance (4, 5). $CD4^+CD25^+$ T_{REG} cells have been detected mainly in lymphoid sites including thymus, lymph nodes, and spleen. Because numerous studies have demonstrated a capacity of T_{REG} cells to prevent the induction of immune responses and because suppression requires direct cell-cell contact with responder T cells or APCs, it is conceivable that T_{REG} cells act as central regulators within lymphoid tissues (6–8).

The gut-associated lymphoid tissue can be divided into effector sites, which consist of lymphocytes scattered throughout the epithelium and lamina propria (LP) of the mucosa and organized lymphoid tissues (inductive sites) that are responsible for the induction phase of the immune response (1, 9). These include Peyer's patches (PPs), mesenteric lymph nodes (MLNs), and isolated lymphoid follicles (ILFs). It is thought that presentation of Ags to immune naive and effector cells is concentrated at these inductive sites of organized mucosal lymphoid follicles, and thus APCs tune the delicate balance between intestinal immune tolerance and inflammation.

In addition to the inductive sites for the development of colitis, however, it also remains unclear where $CD4^+CD25^+$ T_{REG} cells suppress the development of colitis. Although it is reasonable to hypothesize that mechanisms for the induction, maintenance, and suppression of colitis would be centrally controlled by $CD4^+CD25^+$ T_{REG} cells in the inductive sites, we question in this study whether these inductive sites are solely involved in the induction and suppression of intestinal inflammation because we recently demonstrated that human intestinal LP $CD4^+CD25^{bright}$ T cells as well as peripheral $CD4^+CD25^{bright}$ T cells obtained from normal individuals possess T_{REG} activity in vitro (10). Consistent with our previous report, it has been recently reported that $CD4^+CD25^+$ T_{REG} cells were detected in peripheral tissues and at sites of ongoing immune responses such as synovial fluid from rheumatoid arthritis patients (11), tumors (12), transplants (13), skin lesions in mice infected with *Leishmania major* (14), lungs from mice infected with *Pneumocystis carinii* (15), islets of Langerhans in diabetes models (16), and lesions in delayed-type hypersensitivity models (17) as well as in inflamed mucosa in colitic mice (8, 18). In the present study, we conducted a series of the adoptive transfer experiments focusing on intestinal

*Department of Gastroenterology and Hepatology, Graduate School, Tokyo Medical and Dental University, Tokyo, Japan; †Department of Microbiology and Immunology, Nihon University School of Density at Matsudo, Matsudo, Japan; and ‡Department of Microbiology and Immunology, Division of Mucosal Immunology, Institute of Medical Science, University of Tokyo, Tokyo, Japan

Received for publication May 18, 2006. Accepted for publication January 17, 2007.

The costs of publication of this article were defrayed in part by the payment of page charges. This article must therefore be hereby marked *advertisement* in accordance with 18 U.S.C. Section 1734 solely to indicate this fact.

[1] This study was supported in part by grants-in-aid for Scientific Research, Scientific Research on Priority Areas, Exploratory Research and Creative Scientific Research from the Japanese Ministry of Education, Culture, Sports, Science and Technology; the Japanese Ministry of Health, Labor and Welfare; the Japan Medical Association; Foundation for Advancement of International Science; Terumo Life Science Foundation; Ohyama Health Foundation; Yakult Bio-Science Foundation; and Research Fund of Mitsukoshi Health and Welfare Foundation.

[2] Address correspondence and reprint requests to Dr. Takanori Kanai, Department of Gastroenterology and Hepatology, Tokyo Medical and Dental University, 1-5-45 Yushima, Bunkyo-ku, Tokyo 113-8519, Japan. E-mail address: taka.gast@tmd.ac.jp

[3] Abbreviations used in this paper: T_{REG}, regulatory T; LP, lamina propria; PP, Peyer's patch; MLN, mesenteric lymph node; ILF, isolated lymphoid follicle; GITR, glucocorticoid-induced TNFR; LT, lymphotoxin.

LP $CD4^+CD25^+$ T cells to understand where and how $CD4^+CD25^+$ T_{REG} cells control the mucosal immune system in vivo.

Materials and Methods

Animals

Female BALB/c, C.B-17 SCID, and C57BL/6-Ly5.2 mice were purchased from Japan CLEA. C57BL/6-Ly5.1 and C57BL/6-Ly5.2 Rag2-deficient ($Rag2^{-/-}$) mice were obtained from Taconic Farms. Ly5.2 background lymphotoxin (LT)α-deficient ($LT\alpha^{-/-}$) mice were purchased from The Jackson Laboratory. $LT\alpha^{-/-}$ mice were intercrossed into $Rag2^{-/-}$ mice to generate $LT\alpha^{+/+} \times Rag2^{-/-}$ and $LT\alpha^{-/-} \times Rag2^{-/-}$ mice in the Animal Care Facility of Tokyo Medical and Dental University. Mice were maintained under specific pathogen-free conditions in the Animal Care Facility of Tokyo Medical and Dental University. Donors and littermate recipients were used at 6–12 wk of age. All experiments were approved by the regional animal study committees and were done according to institutional guidelines and Home Office regulations.

Abs and reagents

The following mAbs except DTA-1, biotinylated anti-mouse glucocorticoid-induced TNFR (GITR; eBioscience) and FJK-16s, PE-conjugated anti-mouse Foxp3 (eBioscience) were obtained from BD Pharmingen for purification of cell populations and flow cytometry analysis: PE-conjugated anti-mouse CD4 (RM4-5), PE-Cy5- and allophycocyanin-conjugated anti-mouse CD4 (L3T4), FITC-conjugated anti-mouse CD25 (7D4), PE-conjugated anti-mouse CD25 (PC61), PE-conjugated anti-mouse CD103 (α_E integrin) (M290), PE-conjugated anti-mouse $\alpha_4\beta_7$ integrin (DATK32), PE-conjugated anti-CTLA-4 (UC10-4F10-11), FITC-conjugated anti-mouse CD45RB (16A), FITC-conjugated anti-mouse Ly5.1 (CD45.1, A20), FITC-conjugated anti-mouse Ly5.2 (CD45.2, 104), and FITC- and PerCP-conjugated anti-mouse CD3 (145-2C11). Biotinylated Abs were detected with PE- or CyChrome-streptavidin (BD Pharmingen).

Purification of T cell subsets

$CD4^+$ T cells were isolated from normal spleen and colon using the anti-CD4 (L3T4) MACS system (Miltenyi Biotec) according to the manufacturer's instructions. To isolate normal LP $CD4^+$ T cells, the entire length of colon was opened longitudinally, washed with PBS, and cut into small pieces. The dissected mucosa was incubated with Ca^{2+}, Mg^{2+}-free HBSS containing 1 mM DTT (Sigma-Aldrich) for 45 min to remove mucus and then treated with 2.0 mg/ml collagenase and 0.01% DNase (both Worthington Biomedical) for 2 h. The cells were pelleted two times through a 40% isotonic Percoll solution, and then subjected to Ficoll-Hypaque density gradient centrifugation (40%/75%). Enriched $CD4^+$ T cells from the spleen and the colon (spleen, 94–97% pure; colon, 80–90%, as estimated by FACSCalibur (BD Biosciences)) were then labeled with PE-conjugated anti-mouse CD4 (RM4-5), FITC-conjugated anti-CD45RB (16A), and FITC-conjugated anti-CD25 (7D4). Subpopulations of $CD4^+$ cells were generated by two-color sorting on FACSVantage (BD Biosciences). All populations were >98.0% pure on reanalysis.

In vivo experimental design

A series of in vivo experiments was conducted to investigate the role of intestinal LP $CD4^+CD25^+$ T cells in the suppression of murine chronic colitis. In Experiment 1, to assess the role of intestinal LP $CD4^+CD25^+$ T cells obtained from normal mice in the protection of colitis, we transferred 3×10^5 splenic $CD4^+CD45RB^{high}$ T cells from normal BALB/c mice with or without 1×10^5 intestinal LP $CD4^+CD25^+$ T cells into syngeneic C.B-17 SCID mice. All recipient SCID mice were sacrificed at 7 wk after transfer. In Experiment 2, to assess the necessity of gut-associated lymphoid tissues including MLNs in the development and the protection of colitis, we transferred 3×10^5 splenic $CD4^+CD45RB^{high}$ T cells from normal C57BL/6-Ly5.2 mice with or without 1×10^5 splenic $CD4^+CD25^+$ T_{REG} cells from C57BL/6-Ly5.1 mice into $LT\alpha^{-/-} \times Rag2^{-/-}$ mice and the control $LT\alpha^{+/+} \times Rag2^{-/-}$ mice. In Experiment 3, to exclude a possible role of spleen in the suppression of colitis in addition to MLNs, we transferred 3×10^5 colitogenic LP $CD4^+$ T cells ($Ly5.2^+$) obtained from established $CD4^+CD45RB^{high}$ T cell-transferred mice (19) with or without 3×10^5 splenic $CD4^+CD25^+$ T_{REG} cells from C57BL/6-Ly5.1 mice into splenectomized $LT\alpha^{-/-} \times Rag2^{-/-}$ and $LT\alpha^{+/+} \times Rag2^{-/-}$ mice.

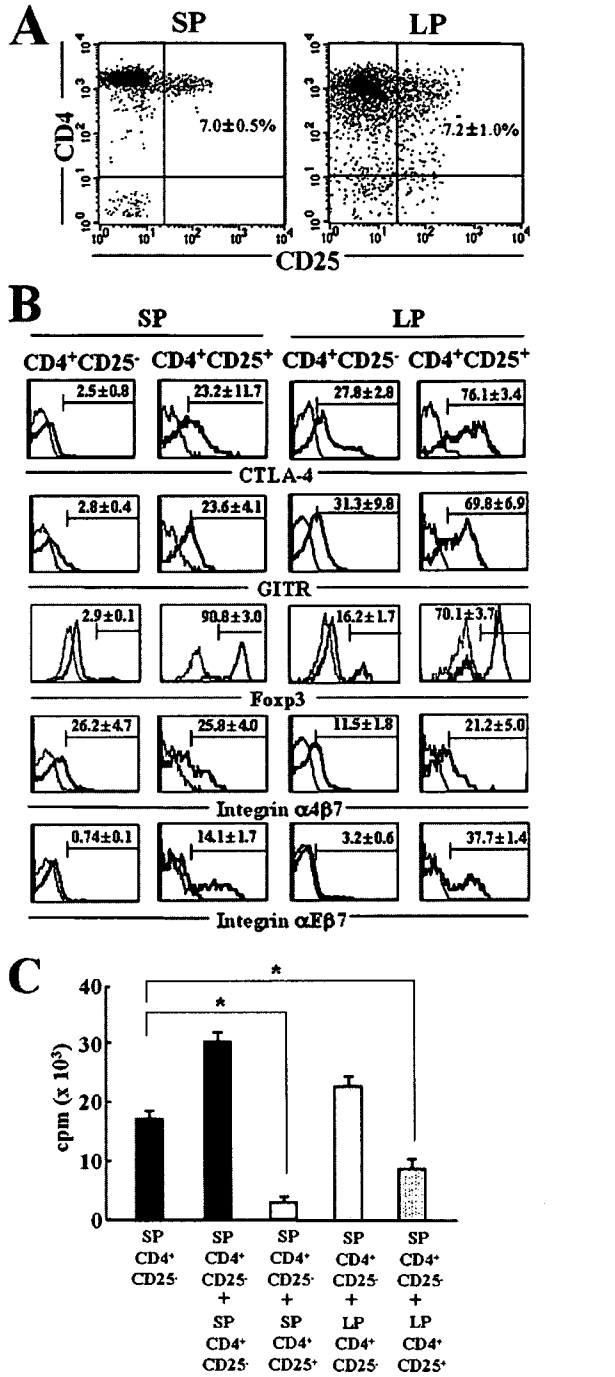

FIGURE 1. Identification and characterization of murine intestinal LP $CD4^+CD25^+$ T cells in terms of T_{REG} cells in vitro. *A*, Freshly isolated murine spleen (SP) and LP mononuclear cells were assessed by a FACSCalibur. Representative sorting gates of the two cell populations, $CD4^+CD25^-$ and $CD4^+CD25^+$, are shown. Percentages in the *upper right quadrant* represent $CD25^+$ cells at indicated site. *B*, Murine intestinal $CD4^+CD25^+$ constitutively express CTLA-4, GITR, and Foxp3 and partially express $\alpha_4\beta_7$ and $\alpha_E\beta_7$ integrins on or in LP $CD4^+CD25^+$ T cells. Thick line histogram represents staining with mAbs against the indicated markers. Thin line histogram represents staining with isotype-matched control IgG. *C*, Murine LP $CD4^+CD25^+$ subsets suppress the proliferation of $CD4^+$ responder T cells in vitro. Splenic $CD4^+CD25^-$/$CD4^+CD25^+$ and LP $CD4^+CD25^-$/$CD4^+CD25^+$ populations were isolated from MACS-purified $CD4^+$ T cells by FACS sorting. The suppressive activity of the indicated subpopulations was determined by coculturing with splenic $CD4^+CD25^-$ responder T cells at a 1:1 ratio of responder to T_{REG} cells in the presence of anti-CD3 mAb and mitomycin C-treated APCs for 72 h. [^{3}H]Thymidine uptake was determined for the last 9 h. Data are represented as the mean ± SD of triplicate samples. *, $p < 0.05$ compared with culture in splenic $CD4^+CD25^-$ responder cells alone.

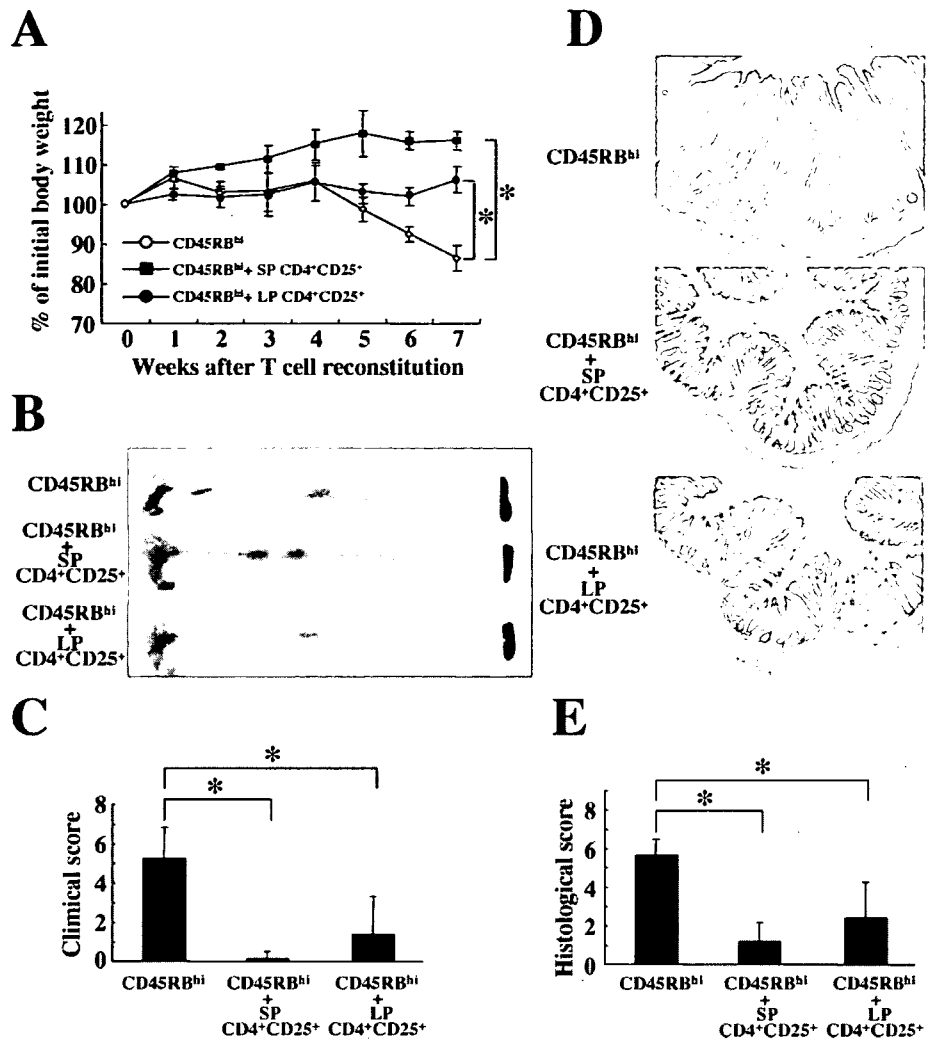

FIGURE 2. Murine intestinal LP $CD4^+$ $CD25^+$ T_{REG} cells as well as splenic $CD4^+$ $CD25^+$ T_{REG} cells inhibit the development of colitis induced by adoptive transfer of $CD4^+CD45RB^{high}$ T cells into SCID mice. Seven SCID mice in each group were injected i.p. with the following T cell subpopulations: 1) splenic $CD4^+CD45RB^{high}$ T cells alone (3×10^5 cells); 2) splenic $CD4^+$ $CD45RB^{high}$ T cells (3×10^5 cells) + splenic $CD4^+CD25^+$ T cells (1×10^5 cells); or 3) splenic $CD4^+CD45RB^{high}$ T cells (3×10^5 cells) + LP $CD4^+CD25^+$ T cells (1×10^5 cells). *A*, Body weight during 7 wk after transfer. *, $p < 0.05$ compared with mice transferred with $CD45RB^{high}$ T cells alone at 7 wk after transfer. *B*, Gross appearance of the colon, MLNs, and spleen from SCID mice transferred with splenic $CD4^+$ $CD45RB^{high}$ T cells alone (*upper*), splenic $CD4^+CD45RB^{high}$ T cells + splenic $CD4^+CD25^+$ T cells (*middle*), or splenic $CD4^+CD45RB^{high}$ T cells + LP $CD4^+CD25^+$ T cells (*lower*) at 7 wk after transfer. *C*, Clinical score at 7 wk after transfer. *, $p < 0.05$ compared with mice transferred with $CD45RB^{high}$ T cells alone. *D*, Histopathology of distal colon at 7 wk after transfer. Original magnification, ×40. *E*, Histological score at 7 wk after transfer. *, $p < 0.05$ compared with mice transferred with $CD45RB^{high}$ T cells alone.

Disease monitoring and clinical scoring

The recipient mice, after T cell transfer, were weighed initially and then three times per week thereafter. They were observed for clinical signs of illness: hunched over appearance, piloerection of the coat, diarrhea, and blood in the stool. Mice were sacrificed at the indicated time point and assessed for a clinical score that is the sum (0–8 points) of four parameters as follows: 0 or 1, hunching and wasting; 0–3, colon thickening (0, no colon thickening; 1, mild thickening; 2, moderate thickening; 3, extensive thickening); 0–3, stool consistency (0, normal beaded stool; 1, soft stool; 2, diarrhea; 3, bloody stool); and an additional point was added if gross blood was noted (19). To monitor the clinical sign during the observed period over time, the disease activity index is defined as the sum (0–5 points) of the described parameters except colon thickening.

Histological examination and immunohistology

Tissue samples were fixed in PBS containing 6% neutral-buffered formalin. Paraffin-embedded sections (5 μm) were stained with H&E. The sections were analyzed without prior knowledge of the type of T cell reconstitution and recipients. The area most affected was graded by the number and severity of lesions. The mean degree of inflammation in the colon was calculated using a modification of a previously described scoring system (19). To detect $CD11c^+$ dendritic cells and $CD4^+$ T cells in the LP, consecutive cryostat sections (6 μm) were fixed and stained with the following rat Abs: purified CD4 (L3T4) and biotinylated anti-CD11c (HL3) (BD Pharmingen). Alexa Fluor 594 goat anti-rat IgG and streptavidin-Alexa Fluor 488 (Molecular Probes) were used as second Abs. All confocal microscopy was conducted on a BioZERO BZ8000 (Keyence).

Flow cytometry

To detect the surface expression of a variety of molecules, isolated splenocytes or LP mononuclear cells were preincubated with an FcγR-blocking mAb (CD16/32, 2.4G2; BD Pharmingen) for 20 min followed by incubation with specific FITC-, PE-, PE-Cy5-, or biotin-labeled Abs for 30 min on ice. Biotinylated Abs were detected with PE- or CyChrome-streptavidin. Intracellular Foxp3 staining was performed with the PE anti-mouse Foxp3 staining set (eBioscience) according to the manufacturer's instructions. Standard two- or three-color flow cytometric analyses were obtained using the FACSCalibur method and CellQuest software. Background fluorescence was assessed by staining with control irrelevant isotype-matched mAbs.

Cytokine ELISA

To measure cytokine production, 1×10^5 LP $CD4^+$ T cells were cultured in 200 μl of culture medium at 37°C in a humidified atmosphere containing 5% CO_2 in 96-well plates (Costar) precoated with 5 μg/ml hamster anti-mouse CD3ε mAb (145-2C11; BD Pharmingen) and 2 μg/ml hamster anti-mouse CD28 mAb (37.51; BD Pharmingen) in PBS overnight at 4°C. Culture supernatants were removed after 48 h and assayed for cytokine production. Cytokine concentrations were determined by specific ELISA per the manufacturer's recommendation (R&D Systems).

In vitro T_{REG} cell activity

LP mononuclear cells and splenocytes from normal BALB/c mice were separated into unfractioned $CD4^+$ T cells, $CD4^+CD25^+$ and $CD4^+CD25^-$ T cells using the anti-CD4 (L3T4) MACS magnetic separation system and/or FACSVantage as described. Cells (5×10^4) and mitomycin C-treated BALB/c $CD4^-$ cells (2×10^5) as APCs were cultured for 72 h in round-bottom 96-well plates in RPMI 1640 supplemented with 10% FCS, 100 IU/ml penicillin, 100 μg/ml streptomycin, 2 mM glutamine, 1 mM sodium pyruvate, and 50 μM 2-ME. Cells were stimulated with 1 μg/ml anti-mouse CD3ε mAb. In coculture experiments, the same number of splenic $CD4^+CD25^+$ or $CD4^+CD25^-$ cells, or LP $CD4^+CD25^+$ or $CD4^+CD25^-$ cells (5×10^4), were added into wells with the fixed dose of splenic $CD4^+CD25^+$ responder cells (5×10^4) and mitomycin C-treated

$CD4^-$ cells (2×10^5), as APCs. Incorporation of [^{3}H]thymidine (1 μCi/well) by proliferating cells was measured during the last 9 h of culture.

Statistical analysis

The results were expressed as the mean ± SD. Groups of data were compared by Mann-Whitney *U* test. Differences were considered to be statistically significant for a value of $p < 0.05$.

Results

Characterization of intestinal LP $CD4^+CD25^+$ in terms of T_{REG} cell in vitro

Paired samples of spleen and colon obtained from normal BALB/c mice were analyzed by flow cytometry for the presence of the $CD4^+CD25^+$ T cells. Consistent with previous reports described, in naturally occurring $CD4^+CD25^+$ T_{REG} cells (4–6), 7.0 ± 0.5% of the splenic $CD4^+$ T cells were $CD25^+$ (Fig. 1*A*). Similarly, 7.2 ± 1.0% of the colonic LP $CD4^+$ T cells were also $CD25^+$ (Fig. 1*A*). Because we previously demonstrated that human intestinal LP $CD4^+CD25^{bright}$ T cells obtained from healthy individuals function as T_{REG} cells in vitro (10), we postulated that intestinal LP as well as MLNs is another important site of regulation of immune responses for intestinal homeostasis in vivo. To prove it, we first assessed whether murine intestinal LP $CD4^+CD25^+$ T cells also express well-known T_{REG} markers, such as CTLA-4, GITR, and Foxp3. Like the control splenic $CD4^+CD25^+$ T cells, the expression of CTLA-4, GITR, and Foxp3 was markedly up-regulated in or on the intestinal LP $CD4^+CD25^+$ T cells (Fig. 1*B*) compared with the paired $CD4^+CD25^-$ T cells. Unexpectedly, but consistent with our human study (10), colonic LP $CD4^+CD25^-$ T cells expressed CTLA-4, albeit to lesser extent compared with the paired colonic $CD4^+CD25^+$ T cells (Fig. 1*B*). To further investigate the migration property of these $CD4^+CD25^+$ T cells, we assessed the expression of $\alpha_4\beta_7/\alpha_E\beta_7$ integrins, which are gut-homing receptors essential to migrate into the colon. As shown in Fig. 1*B*, ~10–30% of cells in each subpopulation expressed $\alpha_4\beta_7$ integrin. In contrast, $\alpha_E\beta_7$ integrin was predominantly expressed on the splenic and LP $CD4^+CD25^+$ T cells, but not on the paired $CD4^+CD25^-$ T cells, indicating that a part of splenic and LP $CD4^+CD25^+$ T cells can directly migrate into the gut.

We next investigated the T_{REG} activity of the murine intestinal LP $CD4^+CD25^+$ T cells by testing their ability to suppress the proliferative responses of the splenic $CD4^+CD25^-$ responder T cells. As shown in Fig. 1*C*, both the splenic and LP $CD4^+CD25^+$ T cells were able to suppress the proliferation of the splenic $CD4^+CD25^-$ responder cells when cocultured at a ratio of 1:1 T_{REG} to responder in the presence of mitomycin C-treated $CD4^-$ APCs and soluble anti-CD3 mAb (Fig. 1*C*), indicating that the LP $CD4^+CD25^+$ T cells were T_{REG} cells as well as the splenic $CD4^+CD25^+$ T cells at least in vitro. As a control, it was shown that titration of the same dose of the splenic or LP $CD4^+CD25^-$ cells with the splenic $CD4^+CD25^-$ responder cells into the cultures did not affect the degree of proliferation, thereby excluding the possibility that an increase in total responder cell number was responsible for the suppressive effect (Fig. 1*C*).

Murine intestinal LP $CD4^+CD25^+$ T cells suppress the development of the $CD4^+CD45RB^{high}$ T cell-transferred colitis

To next analyze the functional role of murine intestinal LP $CD4^+CD25^+$ T cell subset in vivo, we tested the T_{REG} activity of the intestinal LP $CD4^+CD25^+$ T cells using the classical SCID-transferred colitis model induced by the adoptive transfer of $CD4^+CD45RB^{high}$ T cells (19). C.B-17 SCID mice were injected i.p. with one or two subpopulations of sorted $CD4^+$ T cell in PBS: 1) splenic $CD4^+CD45RB^{high}$ T cells alone (3×10^5 per mouse) as a positive control, 2) splenic $CD4^+CD45RB^{high}$ (3×10^5 per mouse) with splenic $CD4^+CD25^+$ T cells (1×10^5) as a negative control, and 3) splenic $CD4^+CD45RB^{high}$ (3×10^5) with LP $CD4^+CD25^+$ T cells (1×10^5). The results clearly demonstrated that control of intestinal inflammation resided predominantly within the intestinal LP $CD4^+CD25^+$ subpopulation as well as the splenic $CD4^+CD25^+$ T cells, as these cells significantly inhibited the development of wasting disease (Fig. 2*A*) and colitis (Fig. 2, *B–E*). Colons from mice reconstituted with a mixture of

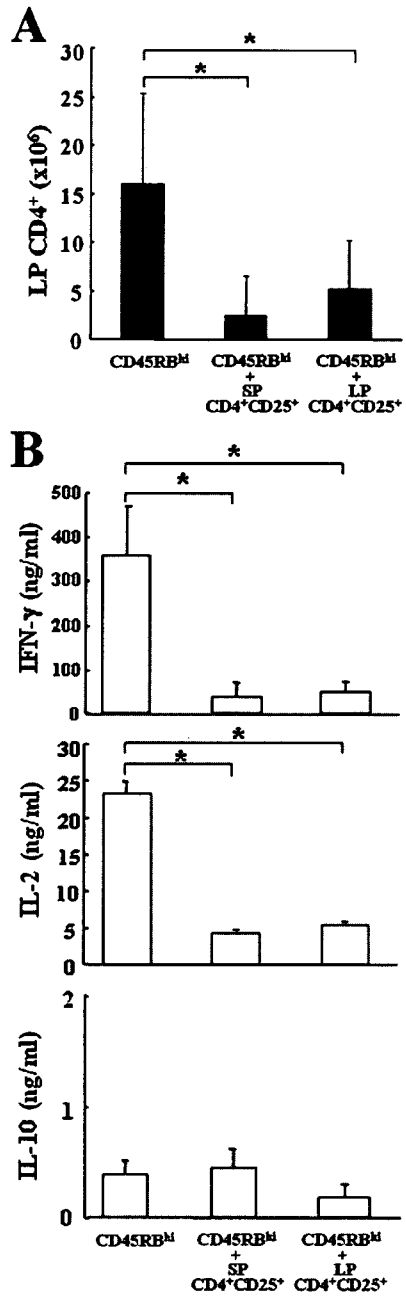

FIGURE 3. Cotransfer of intestinal LP $CD4^+CD25^+$ T_{REG} cells inhibits the expansion of LP $CD4^+$ T cells and Th1 cytokine production in SCID mice transferred with $CD4^+CD45RB^{high}$ T cells. Transfer protocol is described in Fig. 2. *A*, Recovered LP $CD4^+$ T cells at 7 wk after transfer. Data are indicated as the mean ± SD of seven mice in each group. *, $p < 0.05$ compared with mice transferred with $CD45RB^{high}$ T cells alone. *B*, Cytokine production by LP $CD4^+$ T cells. LP $CD4^+$ T cells were stimulated with plate-coated anti-CD3 mAb and soluble anti-CD28 mAb for 72 h. Cytokines in the supernatants were measured by ELISA. Data are indicated as the mean ± SD of seven mice in each group. *, $p < 0.05$ compared with mice transferred with $CD45RB^{high}$ T cells alone.

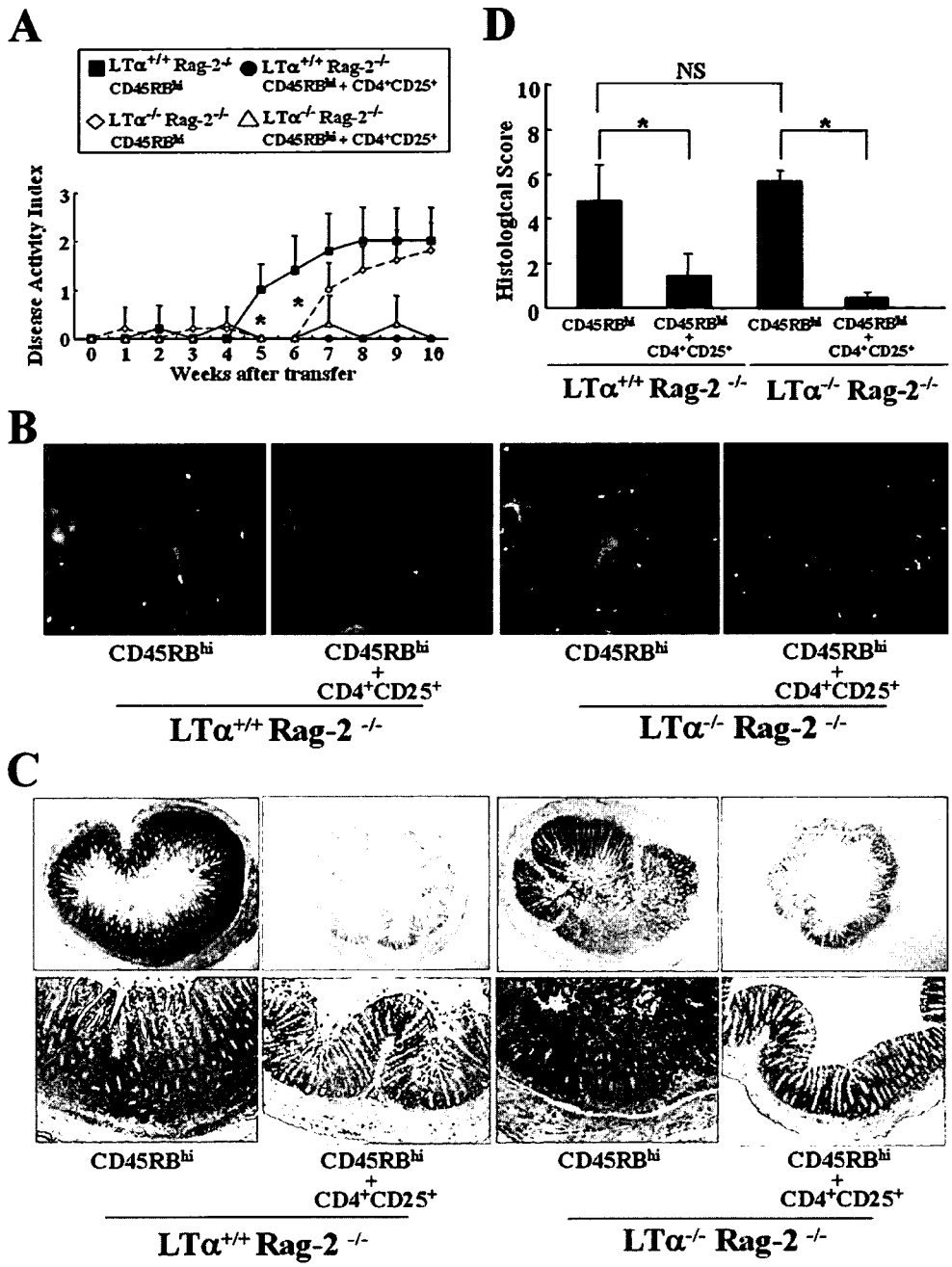

FIGURE 4. Splenic $CD4^+CD25^+$ T_{REG} cells suppress the development of colitis in $LT\alpha^{-/-} \times Rag2^{-/-}$ mice transferred with $CD45RB^{high}$ T cells. $CD4^+CD45RB^{high}$ T cells (3×10^5 cells) from Ly5.2-C57BL/6 congenic mice were injected into Ly5.2 background $LT\alpha^{+/+} \times Rag2^{-/-}$ and $LT\alpha^{-/-} \times Rag2^{-/-}$ mice with or without the cotransfer of 1×10^5 splenic $CD4^+CD25^+$ T_{REG} cells derived from Ly5.1-C57BL/6 mice ($n = 7$ mice per each group). *A*, Disease activity index during 10 wk after transfer. *, $p < 0.05$, $LT\alpha^{+/+} \times Rag2^{-/-}$ mice vs $LT\alpha^{-/-} \times Rag2^{-/-}$ mice, transferred with splenic $CD4^+CD45RB^{high}$ T cells and splenic $CD4^+CD25^+$ T_{REG} cells. *B*, The lack of MLNs in $LT\alpha^{-/-} \times Rag2^{-/-}$ mice. The abdominal MLN area was dissected and examined for the presence or absence of MLNs in $LT\alpha^{-/-} \times Rag2^{-/-}$ mice and $LT\alpha^{+/+} \times Rag2^{-/-}$ mice after adoptive transfer. *C*, Histopathology of distal colon at 10 wk after transfer. Original magnification, ×20 (*top*) and ×100 (*bottom*). *D*, Histological score at 10 wk after transfer. *, $p < 0.05$ compared with the paired $LT\alpha^{+/+} \times Rag2^{-/-}$ or $LT\alpha^{-/-} \times Rag2^{-/-}$ mice transferred with splenic $CD4^+CD45RB^{high}$ T cells alone. NS, Not significant.

$CD4^+CD45RB^{high}$ and LP $CD4^+CD25^+$ T cells exhibited no detectable pathological changes and were indistinguishable from colons from mice reconstituted with a mixture of $CD4^+CD45RB^{high}$ plus splenic $CD4^+CD25^+$ T cells (Fig. 2*B*). In contrast, mice reconstituted with $CD4^+CD45RB^{high}$ cells alone developed wasting disease and severe colitis (Fig. 2). Totally, the assessment of colitis by clinical scores showed a clear difference among three groups (Fig. 2*C*). Clinical score for mice transferred with a mixture of $CD4^+CD45RB^{high}$ and LP $CD4^+CD25^+$ T cells was significantly decreased as compared with that for mice transferred with $CD4^+CD45RB^{high}$ T cells alone. Histological examination showed prominent epithelial hyperplasia with glandular elongation with a massive infiltration of mononuclear cells in the LP of the colon from the control mice transferred with $CD4^+CD45RB^{high}$ T cells alone (Fig. 2*D*). In contrast, the glandular elongation was mostly abrogated and only a few mononuclear cells were observed in the colonic LP from mice reconstituted with a mixture of $CD4^+CD45RB^{high}$ plus splenic or LP $CD4^+CD25^+$ T cells (Fig. 2*D*). This difference was also confirmed by histological scores of multiple colon sections, which were 5.63 ± 0.89 in control mice transferred with $CD4^+CD45RB^{high}$ T cells alone, 1.21 ± 0.97 in mice transferred with $CD4^+CD45RB^{high}$ T cells plus splenic $CD4^+CD25^+$ T cells, and 2.40 ± 1.83 in mice transferred with $CD4^+CD45RB^{high}$ T cells plus LP $CD4^+CD25^+$ T cells ($p < 0.05$, mice transferred with $CD4^+CD45RB^{high}$ T cells alone vs mice transferred with $CD4^+CD45RB^{high}$ T cells plus splenic or LP $CD4^+CD25^+$ T cells) (Fig. 2*E*).

A further quantitative evaluation of $CD4^+$ T cell infiltration was made by isolating LP mononuclear cells from the resected colons. A significantly less number of $CD4^+$ T cells was recovered from the colonic tissue of mice reconstituted with $CD4^+CD45RB^{high}$ and with LP or splenic $CD4^+CD25^+$ T cells as compared with mice reconstituted with $CD4^+CD45RB^{high}$ alone (Fig. 3*A*). To next determine the effect of cotransfer of LP $CD4^+CD25^+$ T cells on Th1/Th2 development, we measured IFN-γ, IL-2, and IL-10 production by anti-CD3/CD28 mAb-stimulated LP $CD4^+$ T cells.

As shown in Fig. 3*B*, production of Th1 cytokines (IFN-γ, IL-2) was significantly reduced in LP CD4+ T cells from the mice transferred with CD4+CD45RB^{high} plus LP or splenic CD4+CD25+ T cells as compared with those transferred with CD4+CD45RB^{high} T cells alone ($p < 0.05$). In contrast, production of IL-10 was not significantly affected among the groups (Fig. 3*B*).

Splenic CD4+CD25+ T cells suppress the development of colitis in LT-α$^{-/-}$ × Rag2$^{-/-}$ mice transferred with CD4+CD45RB^{high} T cells

To further investigate the origin of LP CD4+CD25+ T_{REG} cells and their role in suppressing the development of colitis, we generated LTα$^{-/-}$ × Rag2$^{-/-}$ mice, which lack conventional lymphoid tissues (inductive sites) including MLNs, PPs, and ILFs, as recipients for the adoptive transfer experiments. We excluded the impact of these inductive sites because it was possible that it is essential for LP CD4+CD25+ T_{REG} cells to be instructed to differentiate to gut-homing LP T_{REG} cells in these inductive sites. Before addressing this issue, we first transferred splenic CD4+CD45RB^{high} T cells from normal C57BL/6 mice into LTα$^{-/-}$ × Rag2$^{-/-}$ mice and the littermate control LTα$^{+/+}$ × Rag2$^{-/-}$ mice to assess the role of MLNs as inductive sites in inducing colitis. When CD4+CD45RB^{high} T cells were transferred into the control LTα$^{+/+}$ × Rag2$^{-/-}$ mice, expectedly, the recipients rapidly developed severe wasting disease associated with clinical signs of severe colitis, in particular, weight loss, persistent diarrhea and occasionally also bloody stool and anal prolapses (Fig. 4*A*). When CD4+CD45RB^{high} T cells were transferred into the LTα$^{-/-}$ × Rag2$^{-/-}$ mice, however, the recipients also developed severe wasting chronic colitis despite the delayed onset and kinetics (Fig. 4*A*). Clinical scores in these mice eventually reached almost the same with those in LTα$^{+/+}$ × Rag2$^{-/-}$ mice transferred with CD4+CD45RB^{high} T cells 10 wk after transfer (Fig. 4*A*). The rapid onset of colitis in the recipient LTα$^{+/+}$ × Rag2$^{-/-}$ mice could easily be explained by the existence of MLNs in these mice and migration of effector CD4+ cells primed in the these sites into the colon, but the evidence that the recipient LTα$^{-/-}$ × Rag2$^{-/-}$ mice, albeit delayed, developed colitis indicates that there must be other sites where CD4+ T cells could be primed besides the MLNs. These LTα$^{+/+}$ × Rag2$^{-/-}$ and LTα$^{-/-}$ × Rag2$^{-/-}$ mice transferred with CD4+CD45RB^{high} T cells had an enlarged colon with a significantly thickened wall 10 wk after the transfer (data not shown). At the autopsy of mice, we confirmed that our established LTα$^{-/-}$ × Rag2$^{-/-}$ mice macroscopically lacked MLNs (Fig. 4*B*) and other peripheral LNs (data not shown) in contrast to control LTα$^{+/+}$ × Rag2$^{-/-}$ mice (Fig. 4*B*). Tissue sections from LTα$^{+/+}$ × Rag2$^{-/-}$ and LTα$^{-/-}$ × Rag2$^{-/-}$ mice transferred with CD4+CD45RB^{high} T cells were characterized by inflammatory infiltrate, epithelial hyperplasia, crypt cell damage, and goblet cell depletion (Fig. 4*C*).

Having evidence that LN-null mice developed chronic colitis induced by the adoptive transfer of CD4+CD45RB^{high} T cells, we next asked whether splenic CD4+CD25+ T_{REG} cells can migrate into the LP, and suppress the development of colitis in the absence of MLNs. Expectedly, LTα$^{+/+}$ × Rag2$^{-/-}$ mice transferred with CD4+CD45RB^{high} T cells and splenic CD4+CD25+ T_{REG} cells did not show weight loss and clinical signs of colitis throughout the entire observation period (Fig. 4*A*). Of note, LTα$^{-/-}$ × Rag2$^{-/-}$ mice transferred with a mixture of CD4+CD45RB^{high} T cells and splenic CD4+CD25+ T cells also did not manifest clinical signs of colitis (Fig. 4*A*). Consistent with the lack of clinical signs of colitis, LTα$^{+/+}$ × Rag2$^{-/-}$ or LTα$^{-/-}$ × Rag2$^{-/-}$ recipients cotransferred with CD4+CD45RB^{high} T cells and splenic CD4+CD25+ T cells displayed no histological evidence of intestinal inflammation (Fig. 4*C*). The difference among each group was also confirmed by histological scoring of multiple colon sections, which was 4.85 ± 1.58 in LTα$^{+/+}$ × Rag2$^{-/-}$ mice transferred with CD4+CD45RB^{high} T cells alone, and 1.40 ± 0.96 in LTα$^{+/+}$ × Rag2$^{-/-}$ mice transferred with CD4+CD45RB^{high} T cells plus splenic CD4+CD25+ T cells ($p < 0.05$), and 5.60 ± 0.40 in LTα$^{-/-}$ × Rag2$^{-/-}$ mice transferred with CD4+CD45RB^{high} T cells alone, and 0.43 ± 0.23 in LTα$^{-/-}$ × Rag2$^{-/-}$ mice transferred with CD4+CD45RB^{high} T cells plus splenic CD4+CD25+ T cells ($p < 0.05$) (Fig. 4*D*).

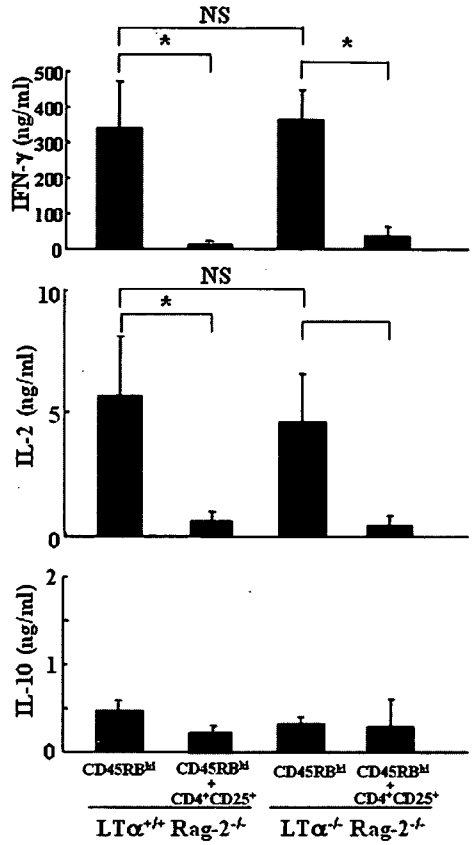

FIGURE 5. Splenic CD4+CD25+ T_{REG} cells suppress the production of Th1 cytokines in LTα$^{-/-}$ × Rag2$^{-/-}$ mice transferred with CD45RB^{high} T cells. CD4+CD45RB^{high} T cells (3 × 10^5 cells) from Ly5.2-C57BL/6 congenic mice were injected into Ly5.2 background LTα$^{+/+}$ × Rag2$^{-/-}$ and LTα$^{-/-}$ × Rag2$^{-/-}$ mice with or without the cotransfer of 1 × 10^5 splenic CD4+CD25+ T_{REG} cells derived from Ly5.1-C57BL/6 mice (n = 7 mice per each group) as described in Fig. 4. Cytokine production by LP CD4+ T cells was measured by specific ELISA. LP CD4+ T cells were stimulated with plate-coated anti-CD3 mAb and soluble anti-CD28 mAb for 72 h. Cytokines in the supernatants were measured by ELISA. Data are indicated as the mean ± SD of seven mice in each group. *, $p < 0.05$ compared with the paired LTα$^{+/+}$ × Rag2$^{-/-}$ or LTα$^{-/-}$ × Rag2$^{-/-}$ mice transferred with splenic CD4+CD45RB^{high} T cells alone. NS, Not significant.

We also examined the cytokine production by LP CD4+ T cells from each group of mice. As shown in Fig. 5, LP CD4+ cells from the LTα$^{+/+}$ × Rag2$^{-/-}$ and LTα$^{-/-}$ × Rag2$^{-/-}$ recipients transferred with CD4+CD45RB^{high} T cells alone produced significantly higher amount of IFN-γ and IL-2 as compared with those transferred with CD4+CD45RB^{high} T cells and splenic CD4+CD25+ T cells upon in vitro anti-CD3/CD28 mAbs stimulation. In contrast, the production of IL-10 was not significantly affected.

Consistent with the reduction in the histological scores by the cotransfer of splenic CD4+CD25+ T cells, there was also a striking reduction in the recovered number of LP CD4+ T cells both in

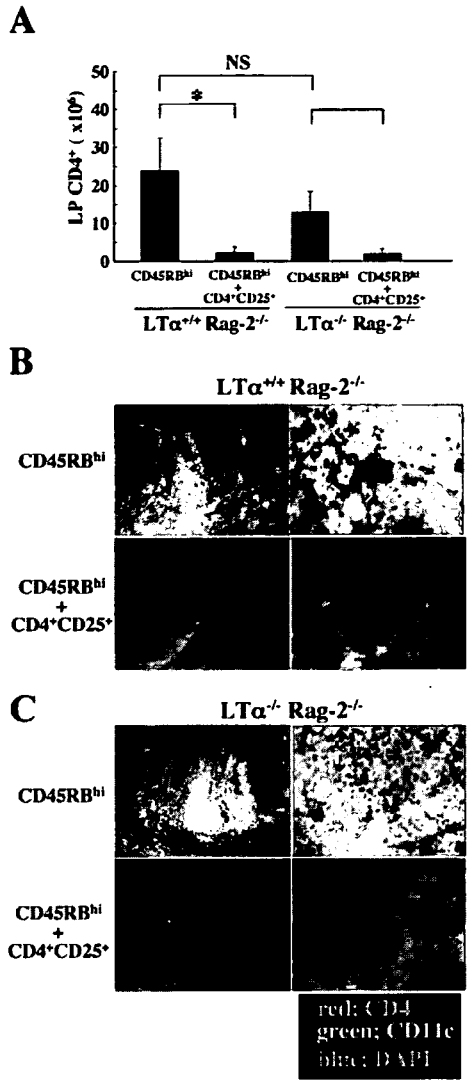

FIGURE 6. Splenic $CD4^+CD25^+$ T_{REG} cells suppress the expansion of pathogenic LP $CD4^+$ T cells in $LT\alpha^{-/-} \times Rag2^{-/-}$ mice transferred with $CD45RB^{high}$ T cells. $CD4^+CD45RB^{high}$ T cells (3×10^5 cells) from Ly5.2-C57BL/6 congenic mice were injected into Ly5.2 background $LT\alpha^{+/+} \times Rag2^{-/-}$ and $LT\alpha^{-/-} \times Rag2^{-/-}$ mice with or without the cotransfer of 1×10^5 splenic $CD4^+CD25^+$ T_{REG} cells derived from Ly5.1-C57BL/6 mice ($n = 7$ mice per each group) as described in Fig. 4. *A*, Recovered LP $CD4^+$ T cells at 10 wk after transfer. Data are indicated as the mean ± SD of seven mice in each group. *, $p < 0.05$ compared with the paired $LT\alpha^{+/+} \times Rag2^{-/-}$ or $LT\alpha^{-/-} \times Rag2^{-/-}$ mice transferred with splenic $CD4^+CD45RB^{high}$ T cells alone. *B*, Distribution of $CD11c^+$ dendritic cells (green) and $CD4^+$ T cells (red) in the colon after adoptive transfer. Original magnification, ×100 (*left*) and ×400 (*right*).

$LT\alpha^{+/+} \times Rag2^{-/-}$ and $LT\alpha^{-/-} \times Rag2^{-/-}$ mice transferred with a mixture of $CD4^+CD45RB^{high}$ T cells and splenic $CD4^+CD25^+$ T cells 10 wk after transfer (Fig. 6*A*) compared with those in the paired recipients transferred with $CD4^+CD45RB^{high}$ T cells alone. To further assess the role of LP as inductive and/or suppressive site, the expression of CD11c in the colon was investigated by immunohistochemistry (Fig. 6*B*). Immunohistochemical analysis of the colons revealed that significant numbers of $CD11c^+$ dendritic cells were surrounded by many $CD4^+$ T cells in both in $LT\alpha^{+/+} \times Rag2^{-/-}$ and $LT\alpha^{-/-} \times Rag2^{-/-}$ mice transferred with $CD4^+CD45RB^{high}$ T cells alone, but with few $CD4^+$ T cells and $CD11c^+$ cells in $LT\alpha^{+/+} \times Rag2^{-/-}$ and $LT\alpha^{-/-} \times Rag2^{-/-}$ mice transferred with a mixture of $CD4^+CD45RB^{high}$ T cells and splenic $CD4^+CD25^+$ T cells (Fig. 6*B*), suggesting a possible role of LP as a site for actively interacting between $CD11c^+$ dendritic cells and $CD4^+$ T cells.

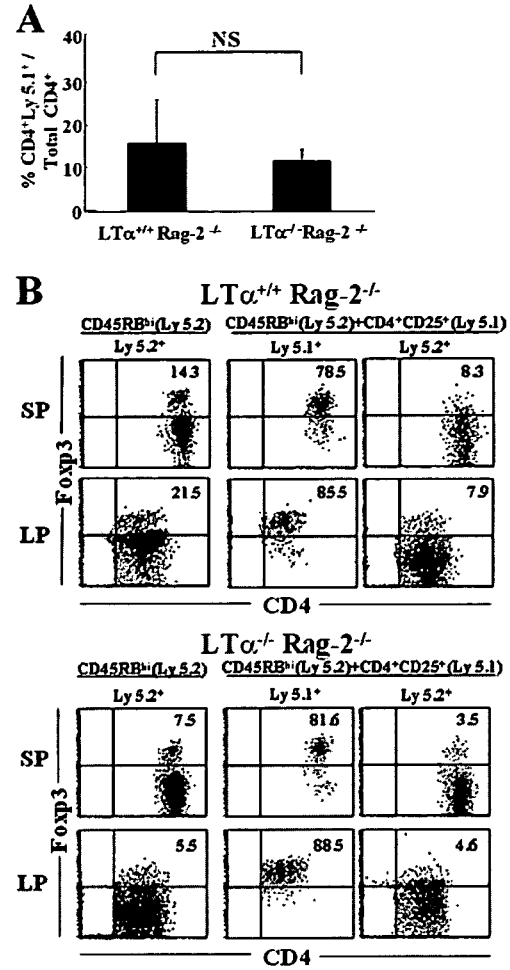

FIGURE 7. Splenic $CD4^+CD25^+$ T_{REG} cells migrate into the colonic LP and are sustained in the LP in $LT\alpha^{-/-} \times Rag2^{-/-}$ mice transferred with $CD45RB^{high}$ T cells. *A*, The ratio of $CD4^+CD25^+$ T_{REG} ($Ly5.1^+$) cells to total $CD4^+$ T cells ($Ly5.1^+$ + $Ly5.2^+$) at 10 wk after transfer was analyzed by gating Ly5.1 or Ly5.2 on $CD4^+$ cells. Results shown are from seven mice per group. NS, Not significant. *B*, Spleen (SP) and LP cells were collected and labeled for Ly5.1, Ly5.2, CD4, and intracellular Foxp3. $Ly5.2^+$ and $Ly5.1^+$ $CD4^+$ cells were gated and analyzed for the presence of converted $Ly5.2^+CD4^+Foxp3^+$ cells and $Ly5.1^+CD4^+Foxp3^+$ cells, respectively. Number in *upper right quadrant* represents the percentage of inducible $CD4^+Foxp3^+$ cells per $CD4^+$ cells.

Splenic $CD4^+CD25^+$ T cells migrate into the intestinal LP in $LT\alpha^{-/-} \times Rag2^{-/-}$ mice

To next assess the in vivo expansion of $CD4^+CD45RB^{high}$ T cells and $CD4^+CD25^+$ T_{REG} cells after adoptive transfer at a 3:1 ratio ($CD4^+CD45RB^{high}$ ($Ly5.2^+$) to $CD4^+CD25^+$ T cells ($Ly5.1^+$)), colonic LP $CD4^+$ cells were analyzed for the ratio of Ly5.2- to Ly5.1-derived cells. As shown in Fig. 7*A*, ~10–15% of total LP $CD4^+$ T cells both in $LT\alpha^{+/+} \times Rag2^{-/-}$ and $LT\alpha^{-/-} \times Rag2^{-/-}$ mice transferred with $CD4^+CD45RB^{high}$ T cells plus splenic $CD4^+CD25^+$ T cells were derived from $Ly5.1^+CD4^+$ $CD25^+$ T cells in the colon. These results suggested that splenic $CD4^+CD25^+$ T cells migrated to the colon, and prevented the development of colitis primarily by inhibiting the expansion and/or infiltration of pathogenic $CD4^+$ T cells in the colon and secondarily by inhibiting the development of pathogenic Th1 cells producing IFN-γ and IL-2.

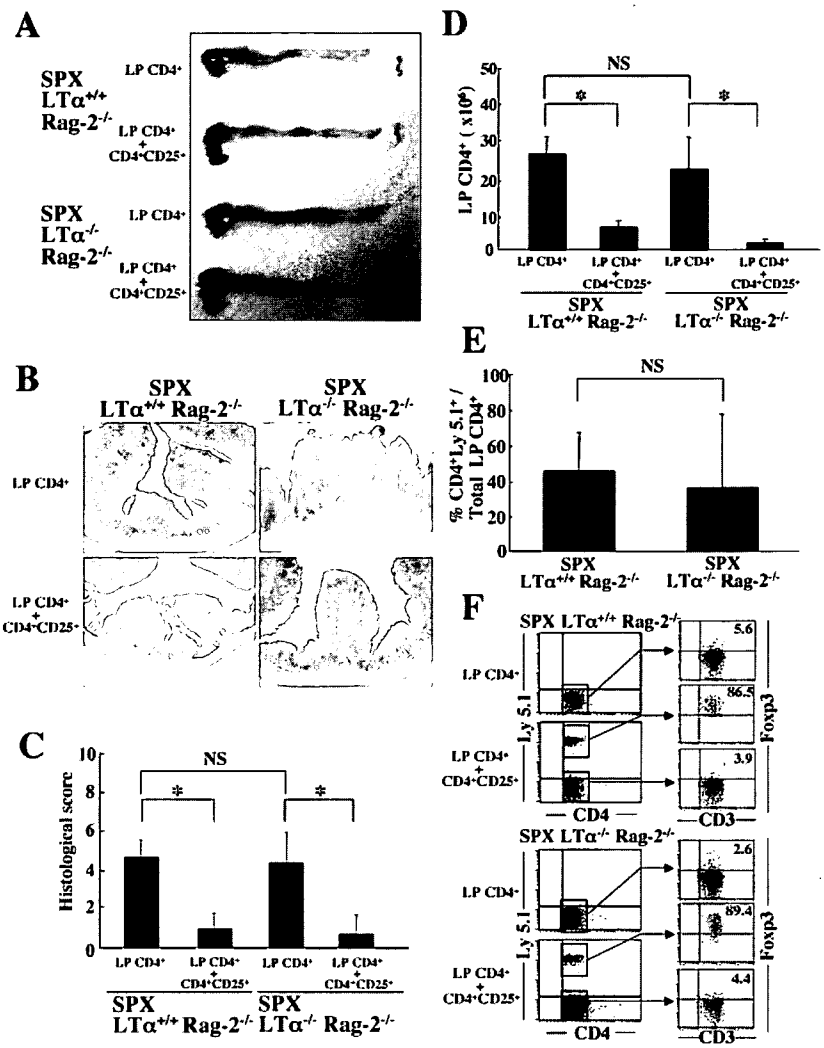

FIGURE 8. Splenic $CD4^+CD25^+$ T_{REG} cells migrate into the gut and inhibit the development of colitis induced by adoptive transfer of colitogenic LP $CD4^+$ T cells into splenectomized (SPX) $LT\alpha^{-/-} \times Rag2^{-/-}$ mice. Seven $Rag2^{-/-}$ mice in each group were injected i.p. with the following T cell subpopulations: 1) colitogenic LP $Ly5.2^+CD4^+$ T cells (3×10^5 cells) into splenectomized $LT\alpha^{+/+} \times Rag2^{-/-}$ mice; 2) colitogenic LP $Ly5.2^+CD4^+$ T cells (3×10^5 cells) + splenic $Ly5.1^+$ $CD4^+CD25^+$ T cells (3×10^5 cells) into splenectomized $LT\alpha^{+/+} \times Rag2^{-/-}$ mice; 3) colitogenic LP $Ly5.2^+CD4^+$ T cells (3×10^5 cells) into splenectomized $LT\alpha^{-/-} \times Rag2^{-/-}$ mice; or 4) colitogenic LP $Ly5.2^+CD4^+$ T cells (3×10^5 cells) + splenic $Ly5.1^+$ $CD4^+CD25^+$ T cells (3×10^5 cells) into splenectomized $LT\alpha^{-/-} \times Rag2^{-/-}$ mice. *A*, Gross appearance of the colon and MLN at 7 wk after transfer. *B*, Histopathology of distal colon at 7 wk after transfer. Original magnification, ×40. *C*, Histological score at 7 wk after transfer. *, $p < 0.05$. *D*, Number of recovered LP $CD4^+$ T cells at 7 wk after transfer. Data are indicated as the mean ± SD of seven mice in each group. *, $p < 0.05$. *E*, Percentage of $CD4^+CD25^+$ T_{REG} ($Ly5.1^+$) cells to total $CD4^+$ T cells ($Ly5.1^+$ + $Ly5.2^+$) at 7 wk after transfer was analyzed by gating Ly5.1 or Ly5.2 on $CD4^+$ cells. Results shown are from seven mice per group. NS, Not significant. *F*, LP cells were collected and labeled for Ly5.1, Ly5.2, CD4, and Foxp3. $Ly5.2^+$ and $Ly5.1^+$ $CD4^+$ cells were gated and analyzed for the presence of $Foxp3^+$ cells. The percentage of induced Foxp3 cells per $CD3^+$ cells is indicated in *upper right quadrant* of enlarged gate.

However, it was also possible that a part of Ly5.2-derived $CD4^+CD45RB^{high}$ T cells was converted into inducible $CD4^+CD25^+$ T_{REG} cells rather than pathogenic $CD4^+$ T cells in the gut. Thus, to evaluate this possibility that the LP $CD4^+CD25^+$ T_{REG} cells are composed of naturally arising $CD4^+CD25^+$ T cells ($Ly5.1^+$), inducible $CD4^+CD25^+$ T cells ($Ly5.2^+$) and pathogenic $CD4^+$ T cells ($Ly5.2^+$), we performed three-color flow cytometry analysis (Fig. 7*B*). In this setting, we stained intracellular Foxp3 because it was difficult to distinguish between activated/pathogenic $CD4^+CD25^+$ T cells and $CD4^+CD25^+$ T_{REG} cells by staining CD25 molecule. Indeed, only ~3–16% of splenic and LP $Ly.5.2^+$ cells were converted into inducible $CD4^+Foxp3^+$ T_{REG} cells in both $LT\alpha^{+/+} \times Rag2^{-/-}$ and $LT\alpha^{-/-} \times Rag2^{-/-}$ mice transferred with $CD4^+CD45RB^{high}$ T cells alone or with a mixture of $CD4^+CD45RB^{high}$ T cells and splenic $CD4^+CD25^+$ T cells, but most Ly.5.1-derived $CD4^+CD25^+$ T_{REG} cells (78–88%) retained Foxp3 in both $LT\alpha^{+/+} \times Rag2^{-/-}$ and $LT\alpha^{-/-} \times Rag2^{-/-}$ mice transferred with a mixture of $CD4^+CD45RB^{high}$ T cells and splenic $CD4^+CD25^+$ T cells (Fig. 7*B*).

Splenic $CD4^+CD25^+$ T cells suppressed the expansion of colitogenic LP $CD4^+$ T cells in the gut

With respect to the site for suppression of effector and memory $CD4^+$ T cells, it was also possible that naturally arising $CD4^+CD25^+$ T cells suppress the activation of $CD4^+CD45RB^{high}$ T cells and the expansion of the differentiated effector $CD4^+$ T cells in the spleen rather than in the gut. To clarify that $CD4^+$ $CD25^+$ T cells suppress the expansion of colitogenic effector and memory $CD4^+$ T cells in the gut, we finally transferred colitogenic LP $CD4^+$ T cells obtained from colitic mice transferred with $CD4^+CD45RB^{high}$ T cells ($Ly5.2^+$) (19) with or without splenic $CD4^+CD25^+$ T cells ($Ly5.1^+$) into splenectomized $LT\alpha^{+/+} \times Rag2^{-/-}$ and $LT\alpha^{-/-} \times Rag2^{-/-}$ mice to exclude the impact of spleen. Both splenectomized $LT\alpha^{+/+} \times Rag2^{-/-}$ and $LT\alpha^{-/-} \times Rag2^{-/-}$ mice transferred with colitic LP $CD4^+$ T cells ($Ly5.2^+$) developed wasting disease (data not shown) and colitis by assessing histological findings (Fig. 8, *A–C*) and the recovered $CD4^+$ cell numbers from the LP (Fig. 8*D*). In contrast, splenectomized $LT\alpha^{+/+} \times Rag2^{-/-}$ and $LT\alpha^{-/-} \times Rag2^{-/-}$ mice transferred with a mixture of colitic LP $CD4^+$ T cells ($Ly5.2^+$) and splenic $CD4^+CD25^+$ T cells ($Ly5.1^+$) at a 1:1 ratio did not develop wasting disease (data not shown) and colitis (Fig. 8, *A–D*). Of note, we found that ~30–40% of LP $CD4^+$ T cells in splenectomized $LT\alpha^{+/+} \times Rag2^{-/-}$ and $LT\alpha^{-/-} \times Rag2^{-/-}$ mice cotransferred with a mixture were derived from $Ly5.1^+$ cells (Fig. 8*E*). Furthermore, we confirmed that $CD4^+Foxp3^+$ T cells residing in the LP were mostly derived from $Ly5.1^+$ population in both splenectomized $LT\alpha^{+/+} \times Rag2^{-/-}$ and $LT\alpha^{-/-} \times Rag2^{-/-}$ mice transferred with a mixture of colitic LP $CD4^+$ T cells ($Ly5.2^+$) and $CD4^+CD25^+$ T cells ($Ly5.1^+$) (Fig. 8*F*), indicating that LP acts as a suppressive site, and spleen is not solely essential to act as a suppressive site to inhibit the expansion of effector $CD4^+$ T cells.

Discussion

In this study, we demonstrate that intestinal LP $CD4^+CD25^+$ T cells residing in normal mice constitutively express CTLA-4, GITR, and Foxp3 and suppress the proliferation of responder $CD4^+$ T cells in vitro. Furthermore, cotransfer of intestinal LP $CD4^+CD25^+$ T cells prevents the development of $CD4^+CD45RB^{high}$ T cell-transferred colitis. Surprisingly, when $LT\alpha^{-/-} \times Rag2^{-/-}$ mice, which lack MLNs, ILFs, and PPs, were transferred with $CD4^+CD45RB^{high}$ T cells, they did develop severe wasting disease and colitis despite the delayed onset and kinetics as compared with the control $LT\alpha^{+/+} \times Rag2^{-/-}$ mice transferred with $CD4^+CD45RB^{high}$ T cells. Of note, splenic $CD4^+CD25^+$ T cells can migrate into the LP, and prevent the development of $CD4^+CD45RB^{high}$ T cell-transferred colitis in MLN-null $LT\alpha^{-/-} \times Rag2^{-/-}$ recipient mice. These results suggest that at least in part intestinal LP $CD4^+CD25^+$ T cells without the instruction by an MLN environment directly migrate into the gut and act as T_{REG} cells, and therefore may contribute to the intestinal immune homeostasis in vivo.

We have recently demonstrated that human $CD4^+CD25^{bright}$ T cells resided in the intestinal LP, expressed CTLA-4, GITR, and Foxp3, and possessed T_{REG} activity in vitro (10). Although the results indicate that these cells might serve as mucosal (nonlymphoid) T_{REG} cells to maintain intestinal homeostasis against many luminal Ags, it was impossible to determine whether they actually suppress the development of colitis in vivo using any human studies. To answer the question, it was necessary to translate into the mouse experimental system. To address this issue, we proceeded with two approaches using the different adoptive transfer experiments in this study. We first directly assessed whether the cotransfer of murine intestinal LP $CD4^+CD25^+$ T cells isolated from normal mice suppress the development of colitis induced by the adoptive transfer of $CD4^+CD45RB^{high}$ T cells into SCID mice. As shown in Fig. 2, we found the clinical score in SCID mice transferred with $CD4^+CD45RB^{high}$ T cells and intestinal LP $CD4^+CD25^+$ T cells at a ratio of 3:1 was significantly decreased as compared with that in SCID mice transferred with $CD4^+CD45RB^{high}$ T cells alone, indicating that the murine intestinal LP $CD4^+CD25^+$ T cells maintain intestinal homeostasis to suppress the development of colitis in vivo. Consistent with this, murine intestinal LP $CD4^+CD25^+$ T cells expressed constitutively CTLA-4, GITR, and Foxp3 and suppressed the proliferation of responder cells in vitro, such as human LP $CD4^+CD25^{bright}$ T cells (10). Furthermore, because we also found that LP $CD4^+CD25^+$ T cells did partially express $\alpha_4\beta_7$ and $\alpha_E\beta_7$ integrins, it is conceivable that these gut-homing receptor-expressing LP $CD4^+CD25^+$ T cells might migrate into the colon from outside of the gut. Although it has been reported that $CD4^+CD25^+$ T_{REG} cells reside in nonlymphoid tissues (10–18), our current data now provide the first experimental evidence that intestinal LP $CD4^+CD25^+$ T cells prevent the development of colitis in vivo.

Having the evidence that the murine intestinal LP $CD4^+CD25^+$ T cells suppressed the development of colitis induced by the adoptive transfer of $CD4^+CD45RB^{high}$ T cells, we next asked whether MLNs are not fully essential for the suppression of colitis by splenic $CD4^+CD25^+$ T cells because it was still possible that 1) a part of the LP $CD4^+CD25^+$ T cells was needed to be instructed in MLNs to differentiate to gut-homing receptor-expressing T_{REG} cells (17) to migrate to the gut, and also possible that 2) the transferred LP $CD4^+CD25^+$ T cells acted as T_{REG} cells in MLNs rather than in the intestine in the first adoptive transfer experiment (Figs. 2 and 3). To address these issues, it was important to assess the $CD4^+CD25^+$ T_{REG} cells without the impact of MLNs, which are thought to be representative inductive and suppressive sites for classical splenic $CD4^+CD25^+$ T_{REG} cells because high expression levels of CD62 ligand enable both naive $CD4^+$ T cells and splenic $CD4^+CD25^+$ T_{REG} cells to efficiently enter the Ag-draining lymph nodes from the bloodstream. As the second approach to address this issue, thus, we generated $LT\alpha^{-/-} \times Rag2^{-/-}$ mice as recipients for the following adoptive transfer experiment. Before starting the experiment, it was unclear whether the $LT\alpha^{-/-} \times Rag2^{-/-}$ mice transferred with $CD4^+CD45RB^{high}$ T cells alone develop colitis, or rather it was likely to envisage that these mice did not develop colitis because MLNs are thought to be very important as inductive sites for the development of colitis. However, it was noteworthy that these mice did develop wasting disease and colitis to a similar extent of the transferred $LT\alpha^{+/+} \times Rag2^{-/-}$ mice 10 wk after transfer, although it took a longer period to establish colitis as compared with the $LT\alpha^{+/+} \times Rag2^{-/-}$ recipients (Fig. 4*A*). Although this fact is actually not a main focus in this study, it is possible that spleen and/or LP are complimentary inductive sites to develop colitis under the absence of MLNs. Consistent with this hypothesis, it has been reported that naive T cells can recruit to the inflamed intestinal mucosa, although these cells are usually excluded from uninflamed nonlymphoid tissues (20). However, the delayed kinetics of the development of colitis in the $LT\alpha^{-/-} \times Rag2^{-/-}$ mice transferred with $CD4^+CD45RB^{high}$ T cells indicates that MLNs are involved in the induction of colitis by their functioning as a professional inductive site. Further study will be needed to address this initial immune response for the development of colitis.

As our focus in this study, we also found that the cotransfer of splenic $CD4^+CD25^+$ T cells obtained from normal mice prevent the development of colitis in $LT\alpha^{-/-} \times Rag2^{-/-}$ mice transferred with $CD4^+CD45RB^{high}$ T cells as well as in $LT\alpha^{+/+} \times Rag2^{-/-}$ recipients, indicating that splenic $CD4^+CD25^+$ T cells can suppress the development of colitis in the absence of MLNs. Moreover, we demonstrated that Ly5.1-$CD4^+CD25^+$ T cells resided in the colon in MLN-null $LT\alpha^{-/-} \times Rag2^{-/-}$ mice cotransferred with Ly5.2-derived $CD4^+CD45RB^{high}$ T cells and Ly5.1-derived splenic $CD4^+CD25^+$ T cells, suggesting that the LP might be a regulatory site between colitogenic effector/memory cells and T_{REG} cells to suppress intestinal inflammation probably as a second line of suppression (17). It was also possible, however, that $CD4^+CD25^+$ T_{REG} cells prevented the expansion of pathogenic effector $CD4^+$ T cells and the migration to the gut in the recipient's spleen rather in the gut. With respect to this issue, we also demonstrated that cotransfer of splenic $CD4^+CD25^+$ T cells prevented the development of colitis induced by adoptive transfer of colitogenic LP $CD4^+$ T cells in splenectomized $LT\alpha^{-/-} \times Rag2^{-/-}$ recipients (Fig. 8). Because colitogenic LP $CD4^+$ T cells that have a phenotype of effector/memory $CD4^+CD44^{high}$ $CD62L^-$ cells (21) should have migrated to the gut and expanded in the gut, it is very likely that splenic $CD4^+CD25^+$ T cells can directly migrate to the gut and suppress the expansion of these colitogenic $CD4^+$ T cells in the gut. With respect to the equilibrium of pathogenic $CD4^+$ T cells and T_{REG} cells, however, further studies will be needed because we found that effector to T_{REG} cell ratio varied by different experimental settings (Figs. 6 and 8).

Finally, it should be discussed the protective mechanism by $CD4^+CD25^+$ T_{REG} cells of this SCID/$Rag2^{-/-}$ colitis model induced by the adoptive transfer of $CD4^+CD45RB^{high}$ T cells from the standpoint of the sites of active suppression. Indeed, Mottet et al. (18) previously demonstrated that not only effector $CD4^+$ T cells but also $CD4^+CD25^+$ T_{REG} cells accumulate in the intestinal LP in addition to the MLNs in the cured SCID mice by retransferring splenic $CD4^+CD25^+$ T cells 3–4 wk after the first transfer

of $CD4^+CD45RB^{high}$ T cells, it remains to be determined whether intestinal inflammation can be suppressed solely by LP or MLN $CD4^+CD25^+$ T_{REG} cells in this setting. In contrast, Denning et al. (8) recently demonstrated that β_7 integrin-deficient ($\beta_7^{-/-}$) $CD4^+CD25^+$ T_{REG} cells that preferentially migrate to MLNs, but are impaired in their ability to migrate to the intestine because of the lack of the gut-homing $\alpha_4\beta_7/\alpha_E\beta_7$ integrin molecules, are capable of preventing intestinal inflammation, suggesting T_{REG} accumulation in the intestine is dispensable for the protection of this colitis model. In this protection protocol, indeed, it is possible that $\beta_7^{+/+}$ $CD4^+CD25^+$ T_{REG} cells are not needed to suppress the development of colitis because $\beta_7^{-/-}$ $CD4^+CD25^+$ T_{REG} cells directly migrate to MLNs and can inhibit naive $CD4^+CD45RB^{high}$ T cell activation and proliferation within Ag-draining MLNs, resulting in suppressing the development of the gut-seeking activated effector $CD4^+$ T cells instructed to express the gut-homing receptors such as $\alpha_4\beta_7/\alpha_E\beta_7$ intergrin. However, it still remains unknown whether mucosal $CD4^+CD25^+$ T_{REG} cells are necessary for the suppression of mucosal pathogenic effector $CD4^+$ T cell ex vivo especially in the therapeutic protocol that can be assessed and whether LP $CD4^+CD25^+$ T_{REG} cells as effector T_{REG} cells can suppress the surrounding LP effector $CD4^+$ T cells ex vivo. In our adoptive transfer experiment using splenectomized MLN-null $LT\alpha^{-/-} \times Rag2^{-/-}$ mice, however, we clearly demonstrated that cotransfer of splenic $CD4^+CD25^+$ T_{REG} cells suppressed the development of colitis despite the lack of spleen and MLNs and found that these T_{REG} cells migrated to the effector sites, in this case, the intestine, suggesting that intestinal LP $CD4^+CD25^+$ T_{REG} cells play an important role at least in part for the suppression of intestinal inflammation in the gut.

In conclusion, our findings showed that intestinal LP functions not only as a critical effector site for inflammatory responses but also as a regulatory (suppressive) site that $CD4^+CD25^+$ T_{REG} cells directly control the pathogenic effector $CD4^+$ cells as a second line of suppression (effector T_{REG}) site together with the MLNs as a first line of suppression (naive T_{REG}) site.

Disclosures

The authors have no financial conflict of interest.

References

1. Mowat, A. M. 2003. Anatomical basis of tolerance and immunity to intestinal antigens. *Nat. Rev. Immunol.* 3: 331–341.
2. Singh, B., S. Read, C. Asseman, V. Malmström, C. Mottet, L. A. Stephens, R. Stepankova, H. Tlaskalova, and F. Powrie. 2001. Control of experimental inflammatory bowel disease by regulatory T cells. *Immunol. Rev.* 182: 190–200.
3. Strober, W., I. J. Fuss, and R. S. Blumberg. 2002. The immunology of mucosal models of inflammation. *Annu. Rev. Immunol.* 20: 495–549.
4. Shevach, E. M. 2002. $CD4^+CD25^+$ suppressor T cells: more questions than answers. *Nat. Rev. Immunol.* 2: 389–400.
5. Sakaguchi, S. 2005. Naturally arising Foxp3-expressing $CD25^+CD4^+$ regulatory T cells in immunological tolerance to self and non-self. *Nat. Immunol.* 6: 345–352.
6. Sakaguchi, S. 2004. Naturally arising $CD4^+$ regulatory T cells for immunologic self-tolerance and negative control of immune responses. *Annu. Rev. Immunol.* 22: 531–562.
7. Thornton, A. M., and E. M. Shevach. 2000. Suppressor effector function of $CD4^+CD25^+$ immunoregulatory T cells is antigen nonspecific. *J. Immunol.* 164: 183–190.
8. Denning, T. L., G. Kim, and M. Kronenberg. 2005. Cutting edge: $CD4^+CD25^+$ regulatory T cells impaired for intestinal homing can prevent colitis. *J. Immunol.* 174: 7487–7491.
9. Spahn, T. W., and T. Kucharzik. 2004. Modulating the intestinal immune system: the role of lymphotoxin and GALT organs. *Gut* 53: 456–465.
10. Makita, S., T. Kanai, S. Oshima, K. Uraushihara, T. Totsuka, T. Sawada, T. Nakamura, K. Koganei, T. Fukushima, and M. Watanabe. 2004. $CD4^+CD25^{bright}$ T cells in human intestinal lamina propria as regulatory cells. *J. Immunol.* 173: 3119–3130.
11. Cao, D., V. Malmström, C. Baecher-Allan, D. Hafler, L. Klareskog, and C. Trollmo. 2003. Isolation and functional characterization of regulatory $CD25^{bright}CD4^+$ T cells from the target organ of patients with rheumatoid arthritis. *Eur. J. Immunol.* 33: 215–223.
12. Curiel, T. J., G. Coukos, L. Zou, X. Alvarez, P. Cheng, P. Mottram, M. Evdemon-Hogan, J. R. Conejo-Garcia, L. Zhang, M. Burow, et al. 2004. Specific recruitment of regulatory T cells in ovarian carcinoma fosters immune privilege and predicts reduced survival. *Nat. Med.* 10: 942–949.
13. Graca, L., S. P. Cobbold, and H. Waldmann. 2002. Identification of regulatory T cells in tolerated allografts. *J. Exp. Med.* 195: 1641–1646.
14. Belkaid, Y., C. A. Piccirillo, S. Mendez, E. M. Shevach, and D. L. Sacks. 2002. $CD4^+CD25^+$ regulatory T cells control *Leishmania major* persistence and immunity. *Nature* 420: 502–507.
15. Hori, S., T. L. Carvalho, and J. Demengeot. 2002. $CD25^+CD4^+$ regulatory T cells suppress $CD4^+$ T cell-mediated pulmonary heperinflammation driven by *Pneumocystis carinii* in immunodeficient mice. *Eur. J. Immunol.* 32: 1282–1291.
16. Lepault, F., and M. C. Gagnerault. 2000. Characterization of peripheral regulatory $CD4^+$ T cells that prevent diabetes onset in nonobeses diabetic mice. *J. Immunol.* 164: 240–247.
17. Siegmund, K., M. Feuerer, C. Siewert, S. Ghani, U. Haubold, A. Dankof, V. Krenn, M. P. Schön, A. Scheffold, J. B. Lowe, et al. 2005. Migration matters: regulatory T-cell compartmentalization determines suppressive activity in vivo. *Blood* 106: 3097–3104.
18. Mottet, C., H. H. Uhlig, and F. Powrie. 2003. Cutting edge: cure of colitis by $CD4^+CD25^+$ regulatory T cells. *J. Immunol.* 170: 3939–3943.
19. Totsuka, T., T. Kanai, R. Iiyama, K. Uraushihara, M. Yamazaki, R. Okamoto, T. Hibi, K. Tezuka, M. Azuma, H. Akiba, et al. 2003. Ameliorating effect of anti-inducible costimulator monoclonal antibody in a murine model of chronic colitis. *Gastroenterology* 124: 410–421.
20. Weninger, W., H. S. Carlsen, M. Goodarzi, F. Moazed, M. A. Crowley, E. S. Baekkevold, L. L. Cavanagh, and U. H. von Andrian. 2003. Naive T cell recruitment to nonlymphoid tissues: a role for endothelium-expressed CC chemokine ligand 21 in autoimmune disease and lymphoid neogenesis. *J. Immunol.* 170: 4638–4648.
21. Kanai, T., K. Tanimoto, Y. Nemoto, R. Fujii, S. Makita, T. Totsuka, and M. Watanabe. 2006. Naturally arising $CD4^+CD25^+$ regulatory T cells suppress the expansion of colitogenic $CD4^+CD44^{high}CD62L^-$ effector memory T cells. *Am. J. Physiol.* 290: G1051–G1058.

Jun Kunisawa
Ichiro Takahashi
Hiroshi Kiyono

Intraepithelial lymphocytes: their shared and divergent immunological behaviors in the small and large intestine

Authors' address
Jun Kunisawa[1], Ichiro Takahashi[2], Hiroshi Kiyono[1]
[1]Division of Mucosal Immunology, Department of Microbiology and Immunology, The Institute of Medical Science, The University of Tokyo, Core Research for Evolutional Science and Technology (CREST), Japan Science and Technology Corporation (JST), Tokyo, Japan.
[2]Department of Mucosal Immunology, Graduate School of Biomedical Sciences, Hiroshima University, Hiroshima, Japan.

Correspondence to:
Hiroshi Kiyono
Division of Mucosal Immunology
Department of Microbiology and Immunology
The Institute of Medical Science
The University of Tokyo
4-6-1 Shirokanedai, Minato-ku
Tokyo 108-8639, Japan
Tel.: 81-3-5449-5270
Fax: 81-3-5449-5411
E-mail: kiyono@ims.u-tokyo.ac.jp

Acknowledgements
This work was supported by grants from Core Research for Evolutional Science and Technology (CREST) of the Japan Science and Technology Corporation (JST); the Ministry of Education, Science, Sports, and Culture; the Ministry of Health and Welfare in Japan; and Uehara Memorial Foundation in Japan. Our thanks are extended to Dr K. McGhee for editorial help.

Immunological Reviews 2007
Vol. 215: 136–153

Immunological Reviews
0105-2896

Summary: At the front line of the body's immunological defense system, the gastrointestinal tract faces a large number of food-derived antigens, allergens, and nutrients, as well as commensal and pathogenic microorganisms. To maintain intestinal homeostasis, the gut immune system regulates two opposite immunological reactions: immune activation and quiescence. With their versatile immunological features, intraepithelial lymphocytes (IELs) play an important role in this regulation. IELs are mainly composed of T cells, but these T cells are immunologically distinct from peripheral T cells. Not only do IELs differ immunologically from peripheral T cells but they are also comprised of heterogeneous populations showing different phenotypes and immunological functions, as well as trafficking and developmental pathways. Though IELs in the small and large intestine share common features, they have also developed differences as they adjust to the two different environments. This review seeks to shed light on the immunological diversity of small and large intestinal IELs.

Keywords: *intraepithelial T lymphocyte (IEL), small and large intestines, development trafficking, classical and non-classical MHC*

Introduction

Mucosal surfaces of the gastrointestinal and respiratory tracts directly interact with the mucosal lumen, the harshest environment in our body and one that is constantly exposed to many foreign antigens, including food nutrients, allergens, and commensal and pathogenic microorganisms. To protect mucosal sites from these foreign materials and to maintain mucosal homeostasis, the aerodigestive tract is equipped with multiple physical, biological, and immunological barriers.

The acquired-type immunological barrier at the mucosal surface is initiated by the induction of antigen-specific immune responses through mucosa-associated lymphoid tissues (MALT) including the Peyer's patches (PPs), isolated lymphoid follicles (ILFs), and the nasopharynx-associated lymphoid tissues (1, 2). MALT are covered with a follicle-associated epithelium, which

contains antigen-sampling M (microfold) cells that allow for selective transport of antigens from the lumen to underlying antigen-presenting cells such as dendritic cells (DCs) and macrophages (3). These cells present the antigen to T and B cells in MALT, rendering them antigen-primed T and immunoglobulin A (IgA)-committed B cells, respectively. These T and B cells then migrate to effector tissues (e.g. intestinal epithelium, *lamina propria*, and nasal passages) via an immunological intranet known as the common mucosal immune system (CMIS). Because these anatomical and functional characteristics enable MALT to act as inductive tissues for the priming of antigen-specific T- and B-cell responses, they have often been made the target for vaccine delivery (4).

Several physical and biological barriers associated with the innate immune system also protect these sites from microbial invasion and help to maintain their mucosal homeostasis. Closely knit to one another via tight-junction proteins like occludins, claudins, and zonula occludens (5, 6) and characterized by brush-border microvilla as well as a dense mucin layer at the apical site, epithelial cells (ECs) physically bar the entry of pathogenic microorganisms by inhibiting attachment and penetration (7). In addition, they produce antimicrobial peptides such as a β-defensin (7). In addition to these antimicrobial peptides, secretory IgA (S-IgA), the predominant isotype at mucosal sites, is secreted and plays an important role in preventing pathogen invasion (4, 8). S-IgA forms a J-chain-mediated polymeric structure that interacts with the polymeric Ig receptor expressed on mucosal ECs, an interaction that is required for their transport into the lumen (9, 10). S-IgA contributes to both acquired and innate immunity. Acquired immunity, principally mediated by B2 B cells, and innate immunity, mediated by B1 B cells, both play equally important roles in S-IgA production in the murine intestinal lamina propria region (11). The B2 B-cell-mediated S-IgA is mainly derived from the CMIS and thus plays a key role in the recognition of T-dependent antigens, while B1 B cells produce antibodies to T-independent antigen, such as phosphorylcholine, a hapten-like antigen associated with many pathogenic bacteria (1, 2, 12). Based on the undiscriminating reactivity of B1 B-cell-derived S-IgA against commensal and pathogenic microorganisms (1, 2, 12), it has been generally considered that B1 B-cell-derived S-IgA plays a pivotal role in the prevention of attachment of both commensal and pathogenic microorganisms.

Intraepithelial lymphocytes (IELs) play an important role in the maintenance of mucosal homeostasis by actively or negatively regulating mucosal innate and acquired immunity. Residing as single cells among ECs, they monitor for stressed or damaged ECs and express αβ T-cell receptors (TCRs) or γδTCRs, which recognize antigenic peptides presented by conventional major histocompatibility complex (MHC) molecules (13) or by non-classical MHC molecules, respectively (14). In addition to the uniqueness of TCR expression, the developmental pathway and immunological functions of the IELs render them distinctive. Although most previous studies focused on IELs mainly in the small intestine, several lines of evidence have demonstrated that immunological and biological differences between the small and large intestine lead to differences in composition of small and large intestinal IELs as well. This review describes and discusses those features that IELs from the two environments share and those that make them distinct.

IEL subsets in the small and large intestines

Type a and type b IELs in the small and large intestine

IELs are interspersed among ECs in both the small and large intestine, but their frequencies vary, with one IEL for every 4–10 ECs in the small intestine and for every 30–50 ECs in the large intestine (15). In both the small and large intestine, IELs mainly consist of T cells. Two unique characteristics of the IELs allow them to be divided into subsets. First, IELs contain cells expressing the homodimeric form of CD8α (CD8αα), which is only barely detectable in the systemic immune compartments. Second, IELs contain more cells expressing γδTCRs than do peripheral T cells, which almost exclusively express αβTCRs. These unique features allow us to divide IELs into two groups: 'type a', which is also detectable in the blood, lymph, and secondary lymphoid organs including PPs, and 'type b', which is far more prevalent in the mucosal epithelium. Type a mucosal T cells express αβTCRs with CD4 or CD8α, while type b IELs express αβTCRs or γδTCRs with a unique coreceptor, CD8αα, or lack CD8 and CD4 altogether [double negative (DN)]. In addition to the uniqueness of CD8αα and αβ/γδTCR expression, type b IELs can be distinguished from type a IELs because they lack some markers, such as CD2 (16), CD28 (17), cytotoxic T-lymphocyte antigen-4 (18), and Thy-1 (19). Although small and large intestines contain both type a and type b IELs, the ratio between type a and type b IELs differs markedly (*Table* 1). The small intestine is rich in CD8αα IELs, while the large intestine contains very few. For example, 65–75% of the IELs in the small intestine of BALB/c mice are type b IELs (60% are CD8αα, 10% are DN) (*Table* 1). Because about 60–70% of small intestinal type b IELs were $\gamma\delta TCR^+$, 40% of the total IELs in the small intestine can be assumed to be γδTCR+ (*Table* 1). In contrast, CD8αα IELs represent only a minor

Table 1. Different composition of IELs in the small and large intestine*

	Small intestine (total cell number 5.4 ± 1.4 × 10^6 cells), %		Large intestine (total cell number 4.3 ± 1.8 × 10^5 cells), %	
T cell subsets	Among total IELs	Among the subset	Among total IELs	Among the subset
CD8αα	62.7 ± 2.5		4.7 ± 0.6	
αβTCR		35.7 ± 3.1		67.3 ± 2.5
γδTCR		64.0 ± 6.5		32.7 ± 2.5
No TCR		N.D.		N.D.
CD8αβ	15.6 ± 2.0		7.3 ± 1.2	
αβTCR		84.6 ± 3.1		95.6 ± 0.6
γδTCR		N.D.		N.D.
No TCR		15.3 ± 3.0		4.3 ± 0.6
CD4	9.0 ± 1.7		31.0 ± 5.6	
αβTCR		87.3 ± 2.1		98.6 ± 0.6
γδTCR		N.D.		N.D.
No TCR		12.7 ± 2.1		1.7 ± 0.6
DP	7.3 ± 0.6		<0.1%	
αβTCR		52.0 ± 6.1		N/A
γδTCR		2.0 ± 1.0		N/A
No TCR		46.1 ± 5.3		N/A
DN	5.4 ± 1.2		57.3 ± 5.2	
αβTCR		2.7 ± 0.6		5.3 ± 0.6
γδTCR		20.7 ± 3.1		4.3 ± 0.6
No TCR		76.6 ± 3.2		90.4 ± 1.0

N.D., not detectable; N/A, not applicable; type b IEL in italics.
*The data were obtained from female BALB/C mice (7–10 weeks) and represent means ± SD (n = 5).

population in the large intestine (*Table 1*). Alternatively, the percentage of DN IELs in the large intestine is higher than in the small intestine (60% in the large intestine, 15% in the small intestine) (*Table 1*).

Unique features of type a IELs

Although type a IELs exclusively express αβTCRs and the coreceptors CD4 or CD8αβ, traits typical of peripheral T cells, they also differ from conventional T cells in a number of ways. For instance, the ratio of CD8αβ to CD4 in the small intestinal IELs is much higher than in the spleen, while the ratio in the large intestine is similar to that in the spleen. Additionally, in the small but not the large intestine, CD8αα expression can be coexpressed by CD8αβ (20) and CD4 (21) conventional mucosal T cells as well as by single-positive IELs.

Natural-killer-like cells in the intestinal epithelium

An additional unique feature of IELs is the ability of some, the so-called natural killer T (NKT) IELs (22–24), to express NK receptors. The ligand for one of these NK receptors, NKG2D, is the human non-classical MHC molecule MICA/B (MHC class I-chain-related gene A/B), which is predominantly expressed on damaged or transformed ECs (25). Interestingly, γδTCR recognizes the same MICA/B molecules (26, 27), implying that IELs can use both γδTCR and NKG2D to recognize damaged or stressed ECs through MICA.

Also present in the IEL population are TCR^- NK cells whose characteristics differ from those of splenic NK cells (22, 23, 28). Our group previously demonstrated that the cytotoxic effects of NK IELs were enhanced by interleukin-15 (IL-15) (28). IL-15 has also been reported to regulate NKG2D (29) as well as MICA expression (30). Furthermore, it has recently been reported that IL-15 induces CD94 expression and interferon-γ (IFN-γ) and IL-10 production from IELs, allowing them to show Fas-ligand-mediated killing activity (31). Although little has been reported about NK or NKT IELs in the large intestine (24), it is likely that these NK-like IELs directly and/or indirectly interact with ECs for the maintenance of intestinal homeostasis.

Recent thymic emigrants are a novel subclass of IELs

Staton *et al.* (32) have reported that a naive population in IELs is made up of $CD8^+$ recent thymic emigrants (RTEs). In general, naive T cells migrate into the intestine after activation in the gut-associated lymphoid tissue (GALT) [e.g. PPs and mesenteric lymph nodes (MLNs)], but RTEs are distinguished by the ability to migrate into the small intestine without activation (32) (*Fig. 1*). Unlike naive T cells in the periphery, RTEs exclusively express α4β7 integrin, αE integrin, and CCR9, making them gut-tropic T cells (33) (*Fig. 1*). After migrating directly into the intestinal epithelium from the thymus, they begin to proliferate in response to antigen exclusively present in the gut and to show a phenotype similar to that of resident IELs (32). Based on the